Supplementary Information (SI) for Journal of Materials Chemistry A.
This journal is © The Royal Society of Chemistry 2025

Supporting Information for

Single-ion-conducting polymer electrolytes based upon borate-chain step-growth polymers.

Megan Van Vliet,[a] Stephanie L. Wunder,[a] and Michael J. Zdilla*[a]

Contents

FTIR Spectroscopy

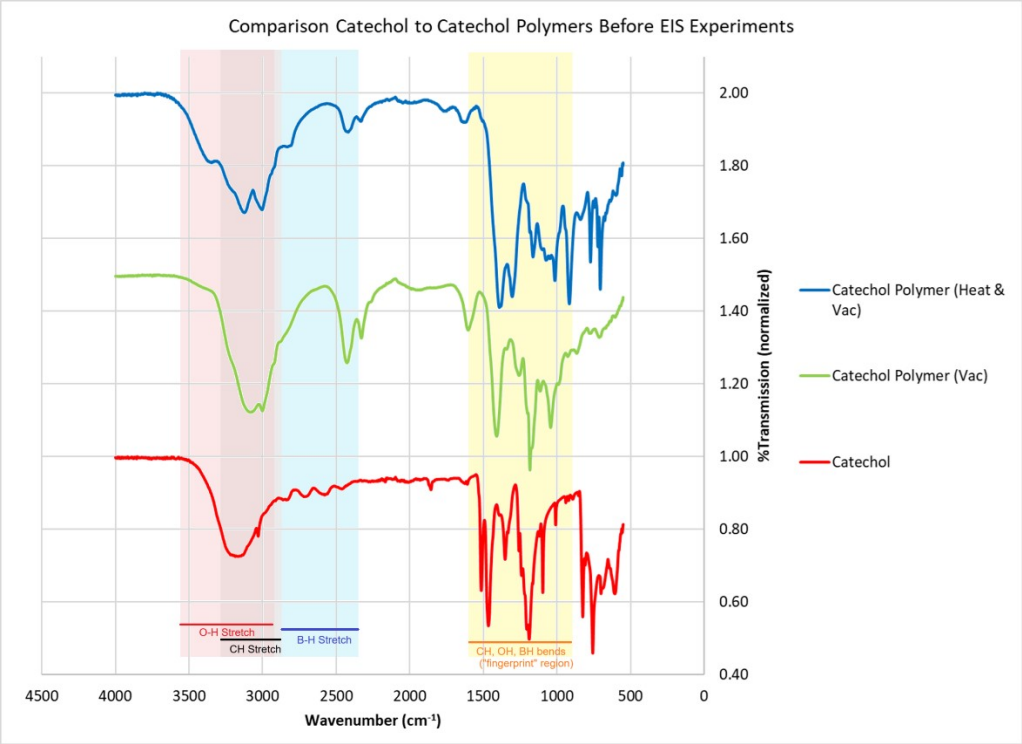

Figure S1. FTIR spectra of catechol precursor and samples of polymer **3-O.**

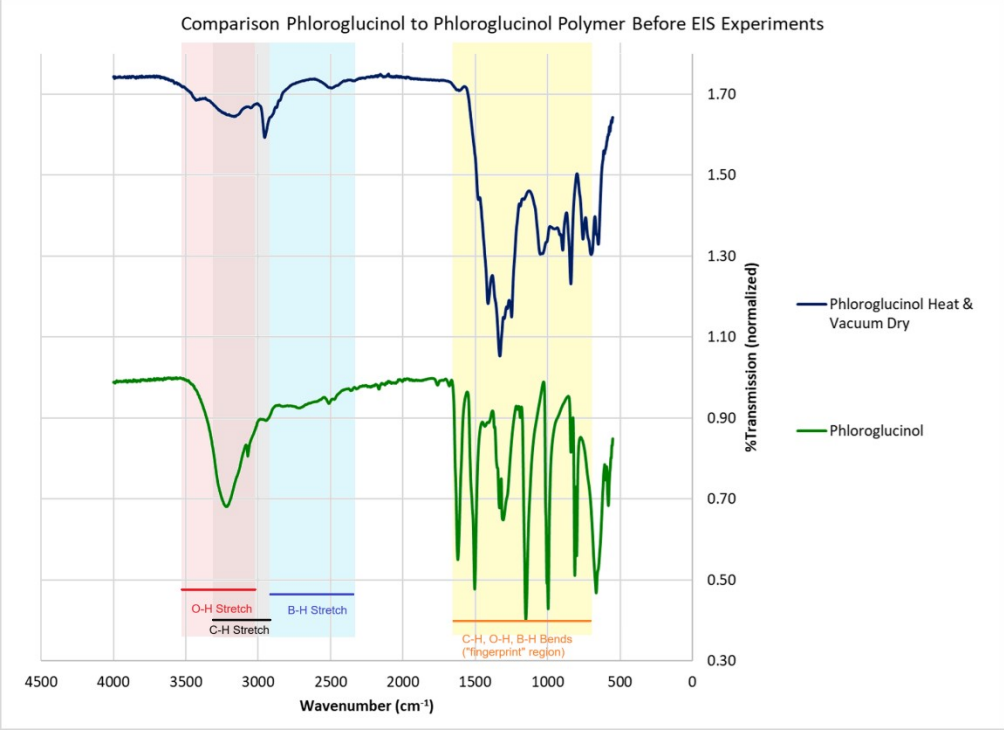

Figure S2. FTIR spectra of phloroglucinol precursor and polymer **4-O.**

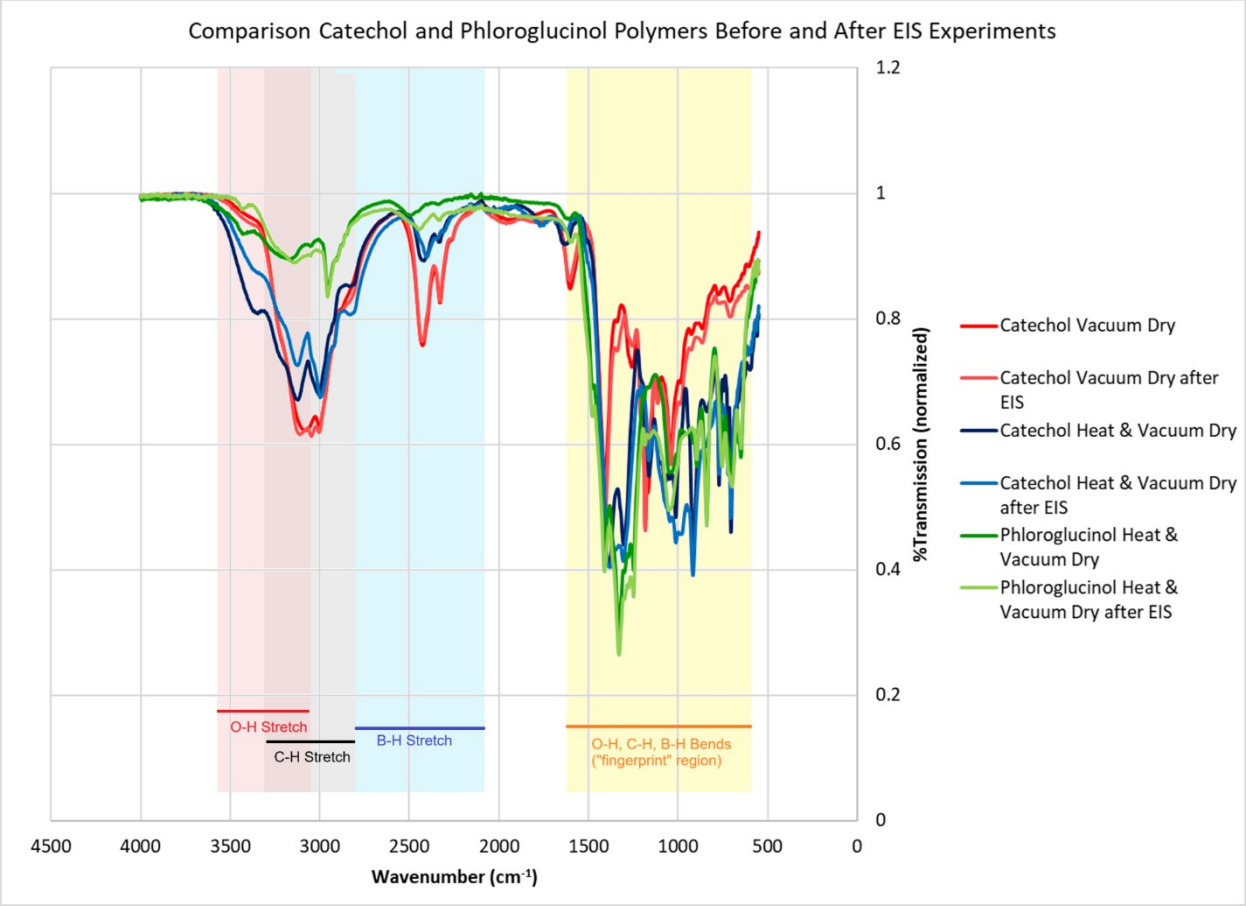

Figure S3: FTIR Spectra of Catechol- and Phloroglucinol-based polym**ers 3-O** and **4-O** before and after Electrochemical Impedance Spectroscopy

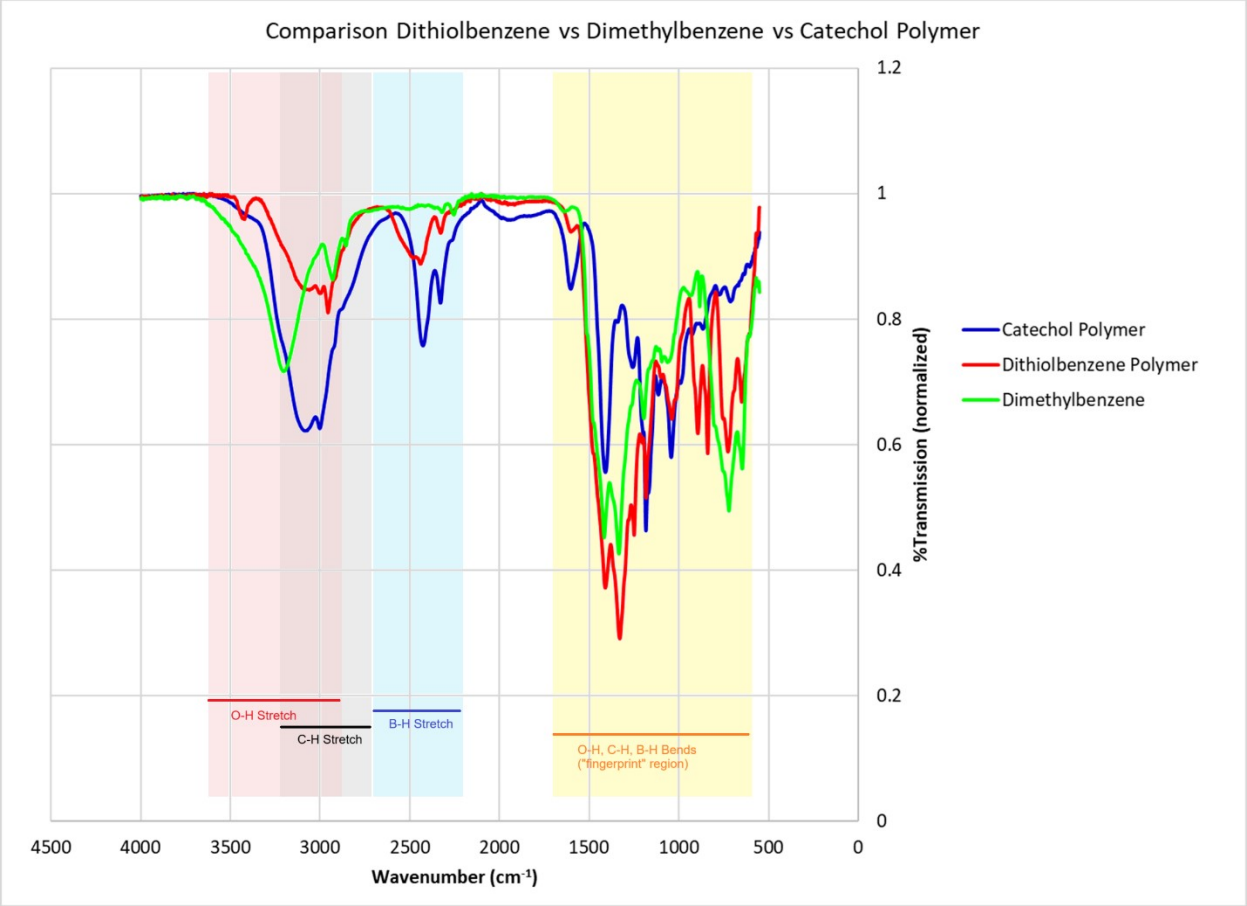

Figure S4: FTIR Spectra of Catechol- and Phloroglucinol-based polymers **3-O, 3-S,** and **3-CH_2.**

Table S1: Common FTIR Signatures from Literature and Observed Experimental Wavenumbers in 3-O and 4-O Pertinent to Aromatics and Boron-containing Molecules[4–10]

Chemical Group	*Literature Wavenumber Range*	*Catechol Reagent*	*Catechol Polymer Vacuum|Heat & Vacuum*	*Phloroglucinol Reagent*	*Phloroglucinol Polymer Heat & Vacuum Dry*
Intermolecular Alcohols	3600-3200 (s,b) 3200-2700 (b)	3490-3050 2840-2460	3200(b)|3250(b) 2800(b)|2820(b)	3470-3080 3220-2720	3640-3017 2955
In-plane O-H Stretch	1350	1350		1330	1330
Aromatic C-H Stretch	3100-3000 (m,s)	3030	3080|3130	3070	
1,4-Disubstituted	3100-3000(w) 2000-1700(w) 1650-1550(m,m) 1150-1100(m,m) 775-700(s,s) 900-800(s)	 1630,1520 1100 700 	3010|3000 2080-1725|2000-1900 1600|1635 1190,1110|1160,1070 770,710|770,710 	3070 1770 1620,1504 1210,1200 800	 1620 1200,1170 755,700
1,3,5-Trisubstituted	950-850 700			840 675	840
Aromatic C-H Stretch	3050	3030		3070	
C-H Bending	860-680(s) 1430-1290	830,760 1400	770|770 1400|1390	840,810,800	
C=C Bending	1700-1500(m,m) 1470	1630,1520 1470	1725,1600|1760,1630	1770,1680 1430	
Out of plane C=C Bending	700	700	710|710	675	
O-Aryl	1220(s) or 1100(m)	1275	 1110|1100	1300 1010	1300 1010
C-O	1150-1050	1100	1040|1050	1150	1050
B-Aryl	1470-1430				1415
B-O	1450-1425 1360-1310 1280-1260 890-860 640-600		 1350|1310 1260 895,865|850 635		 1250 895 650
B-H	2630-2350		2430,2330|2420,2330		2500,2350
B-H scissoring modes	1620-1440 1205-1140 1075-1010		 1000|1010		 960

Table S2. Common FTIR Signatures from Literature and Observed Experimental Wavenumbers in 3-O, 3-S, and 3-CH_2 Pertinent to Aromatics and Boron-containing Molecules[4–10]

Chemical Group	*Literature Wavenumber Range*	*Catechol Polymer (Heat & Vacuum)*	*Dithiobenzene Polymer*	*Dimethylbenzene Polymer*
Intermolecular Alcohols	3600-3200 (s,b) 3200-2700 (b)	3250(b) 2820(b)		
In-plane O-H Stretch	1350			
Aromatic C-H Stretch	3100-3000 (m,s)	3130	3090,2960	3200,2930
1,4-Disubstituted	3100-3000(w) 2000-1700(w) 1650-1550(m,m) 1150-1100(m,m) 790-700(s,s) 900-800(s)	3000 2000-1900 1635 1160,1070 770,710	3000 2000 1600 840	 1640 820
Aromatic C-H Stretch	3050			
C-H Bending	860-680(s) 1430-1290	770 1390	760 1410,1330	760,650 1420,1340
C=C Bending	1700-1500(m,m) 1470	1760,1630		
Out of plane C=C Bending	700	710	720	730
O-Aryl	1220(s) or 1100(m)	1100		
C-O	1150-1050	1050		
B-O or *B-C vibrations	1450-1425 1360-1310 1280-1260 890-860	 1310 1260 850		1420* 1340* 880*
B-H	2630-2350	2420,2330	2475,2325	2330,2260
B-H scissoring modes	1620-1440 1205-1140 1075-1010	 1010	 1180 1005	 1195 1060
BH_2 "wagging"	975-945			950
S-H, thiophenols	2700-2500 (w)		2545	
C-S	710-570 (w) 1300 1275 1025		650 1330 1250 1040	
C=S	1225-1030			
Sulfonamides	3400(s)		3440	

NMR Spectroscopy

In the figures below, the proton and boron NMR are shown for the catechol borohydride polymer and there is strong indication that the lithiated catechol reacts with the boron reagent due to the upfield shift of the aromatic protons (δ 8.66 to δ 7.21) due to the shielding of nuclei. Further, the upfield shift is expected because of the starting material versus polymer functional group polarity. In comparison of alcohol to ether groups (-OH versus -O-), alcohols are high on the polarity scale whereas ethers are low; for reference a polarity index of non-polar pentane scales at 0.0 and polar water scales at 9.0— methanol has a polarity index of 5.1 and ethyl ether is 2.8.[11] Upon polymerization, the atoms become more "shielded" due to the negative formal charge on B, and should shift upfield as the catechol lithiated alcohol groups are then converted into ether linker points for the boron reagent.

Also shown in Figures S5-S8 is the ^{11}B-NMR spectra of the catechol borohydride polymer which have a large range of chemical shifts. Alkyl boranes 90 to 40ppm, borates 30 to 10ppm, BX_3 50 to -20ppm, boron complexes 20 to -80ppm, and BX_4 20 to -120ppm are some typical chemical shifts. The peaks of the catechol borohydride polymer confirm tetravalently coordinated boron centers.

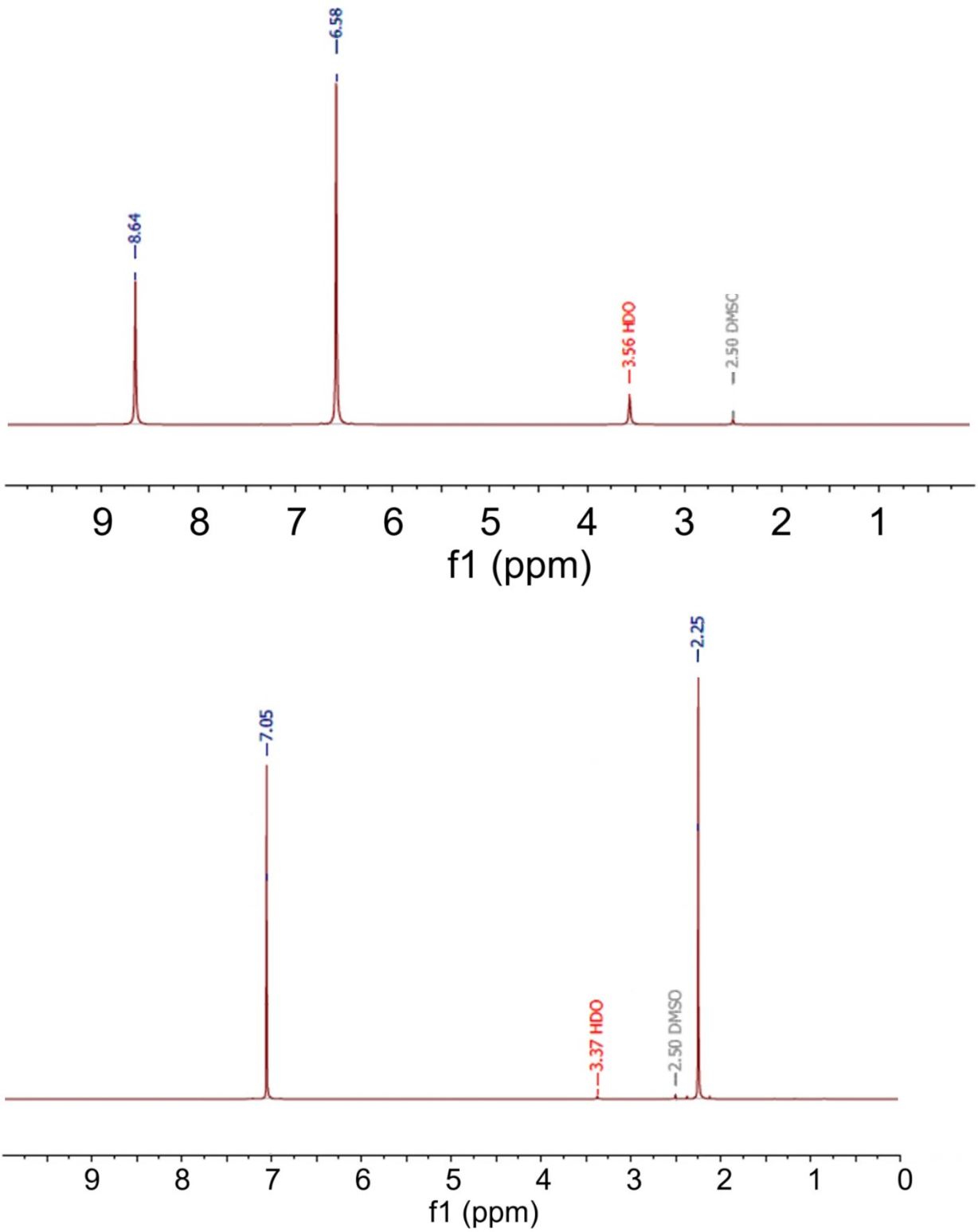

Figure S5: NMR spectra of starting materials. Top: ^{1}H NMR spectrum of 1,4-catechol in DMSO-*d*6. Bottom: ^{1}H NMR spectrum of 1,4-xylene in DMSO-*d*6.

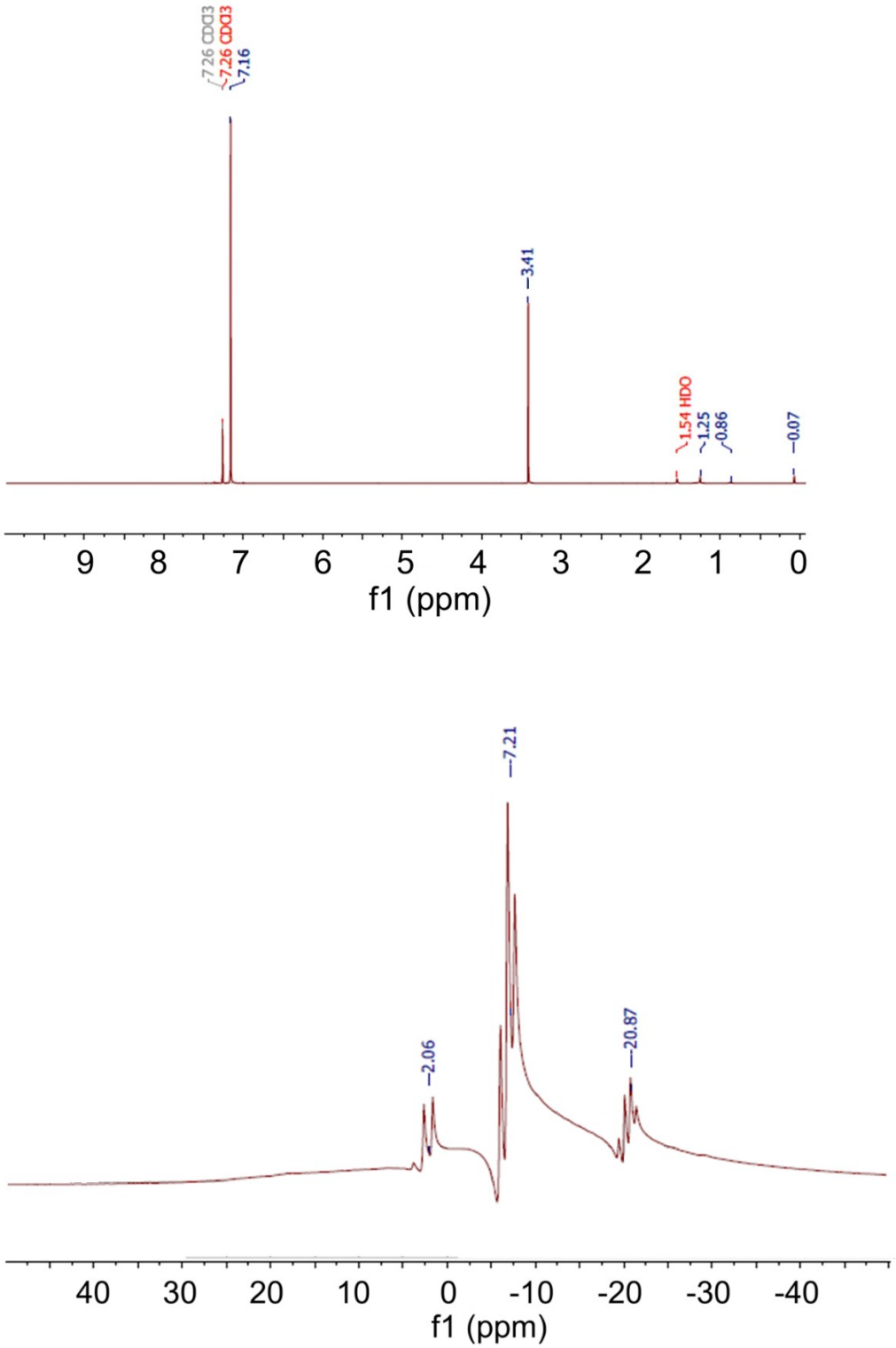

Figure S5 (cont): NMR spectra of starting materials. Top: ^{1}H NMR spectrum of 1,4-dithiobenzene in DCM-*d*. Bottom: ^{11}B NMR spectrum of $BH_2Cl(SMe_2)$ in THF.

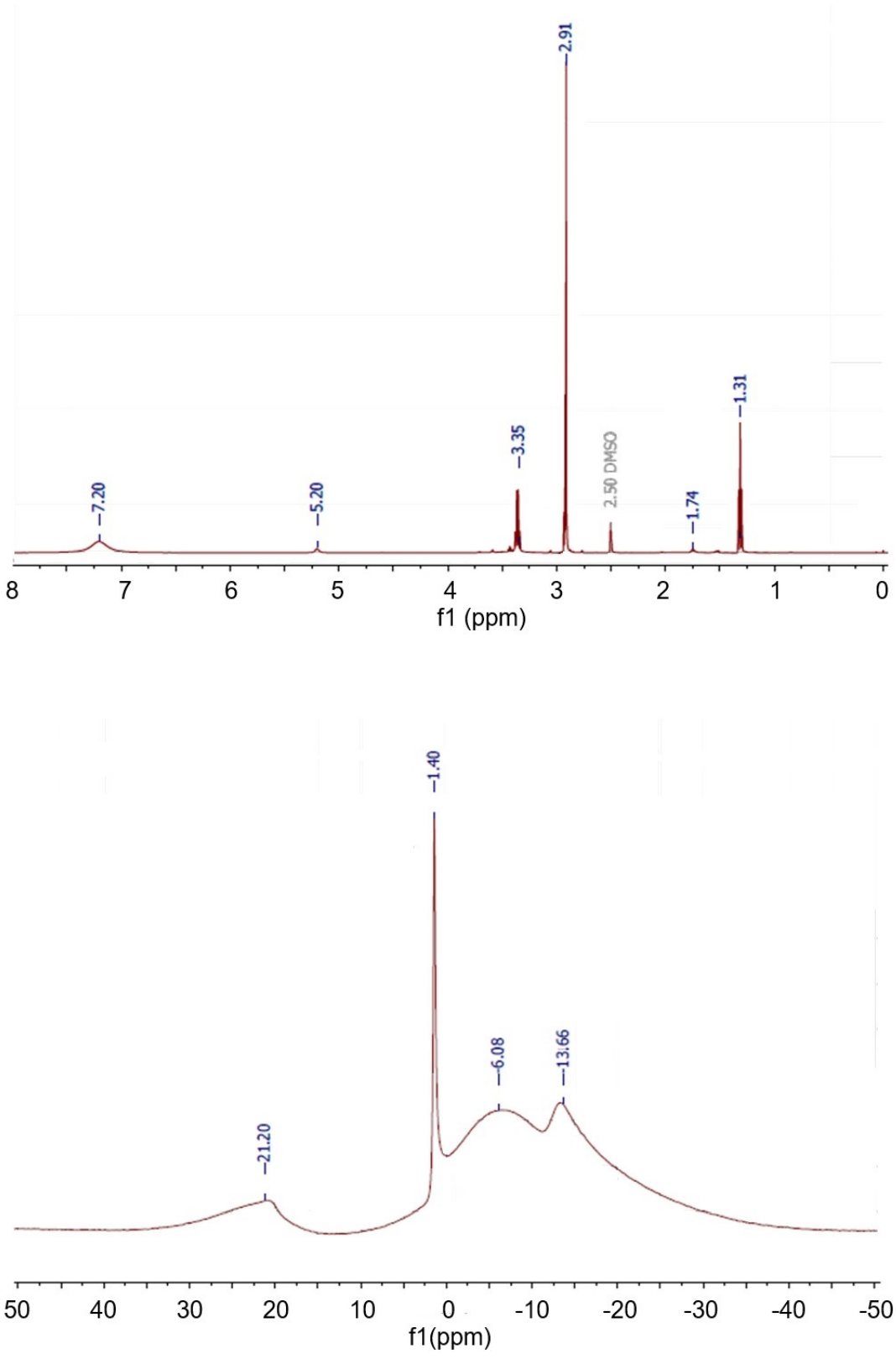

Figure S6: ^{1}H-NMR (top) and ^{11}B NMR (bottom) of Catechol Borohydride Polymer **3-O.**

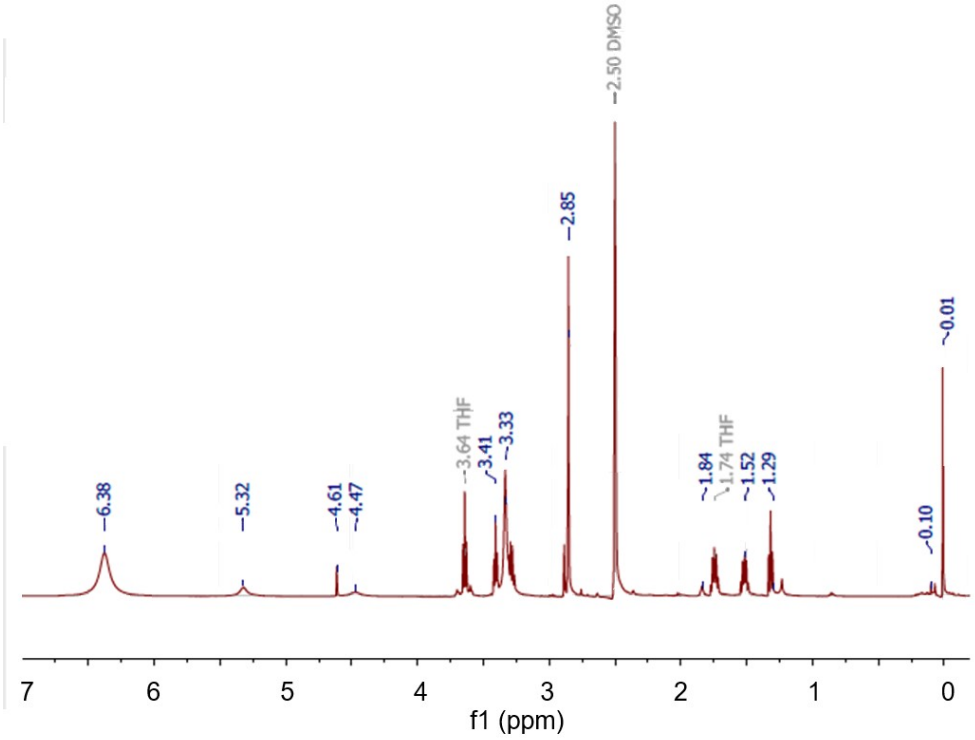

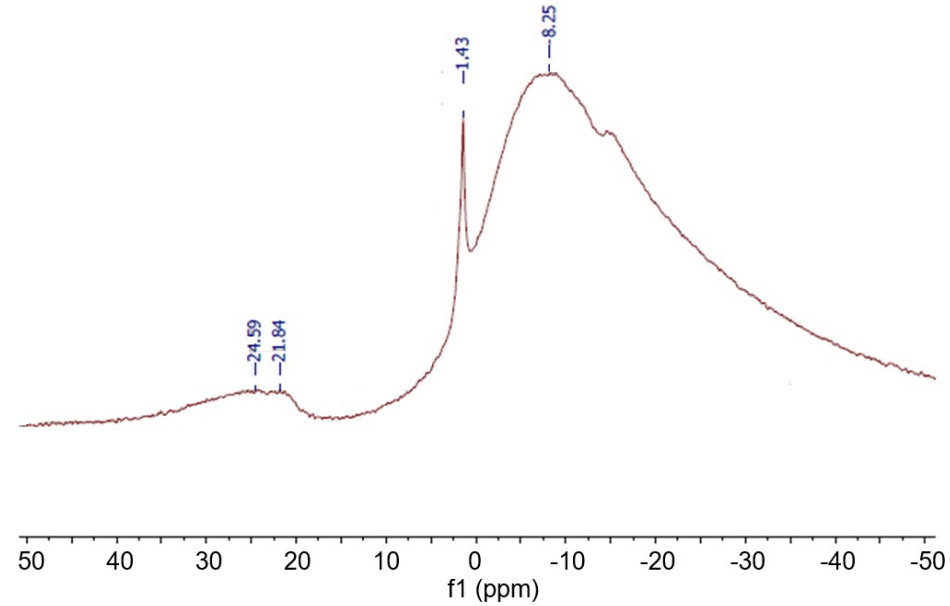

Figure S7. ^{1}H-NMR (top) and ^{11}B NMR (bottom) of 3-S.

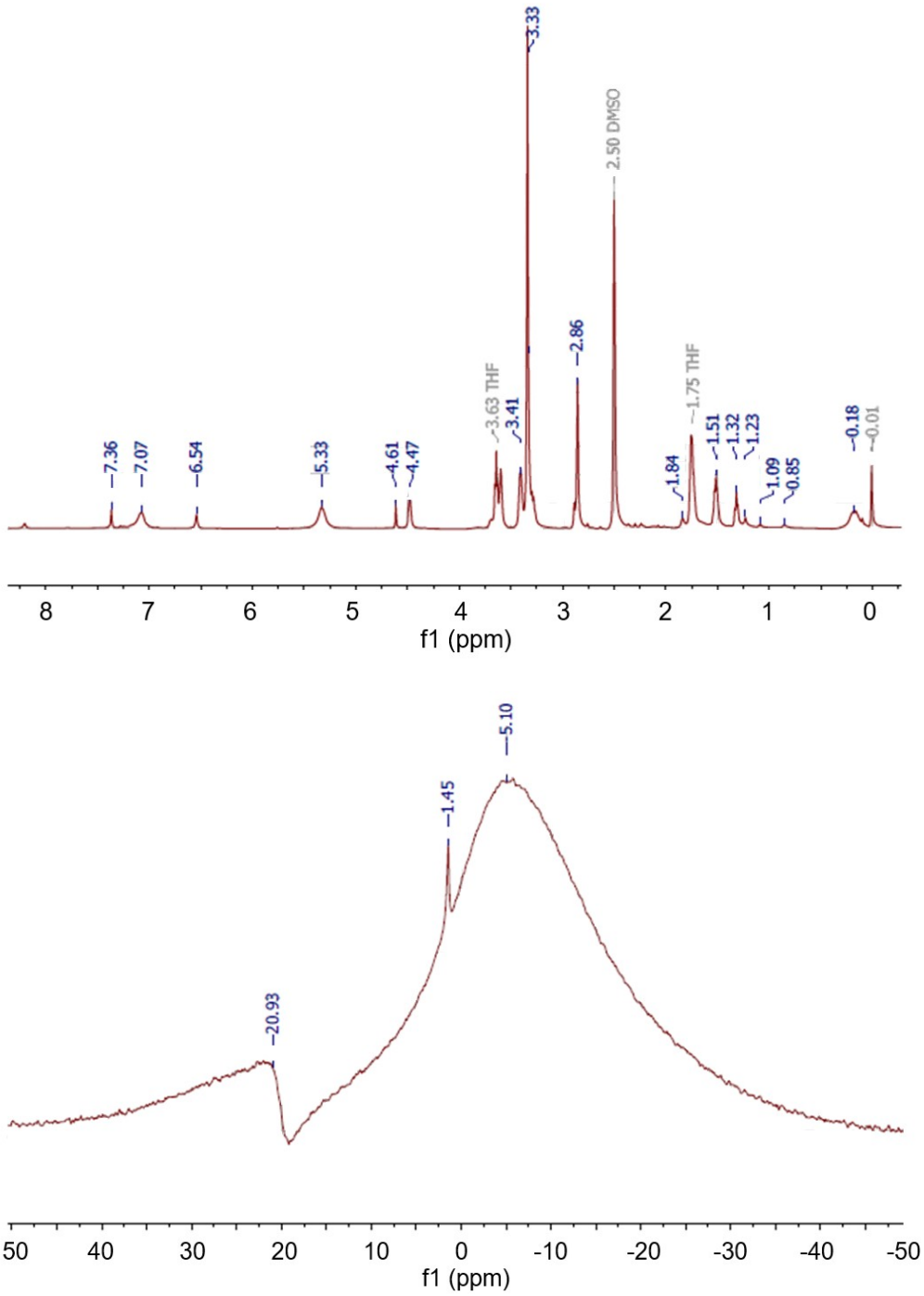

Figure S8. ^{1}H-NMR (top) and ^{11}B NMR (bottom) of 3-CH_2.

GPC

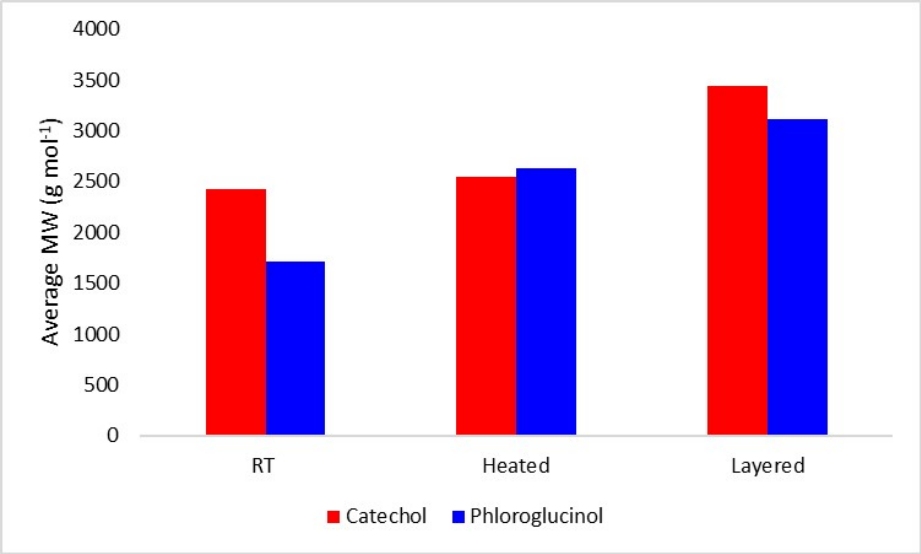

Figure S9. Comparison of Average Molecular Weights of catechol based (**3-O**) and Phloroglucinol-based (**4-O**) borohydride polymers prepared using different synthetic approaches.

	Reaction Conditions	***Molecular Formula for Polymer Unit***	***Molecular Weight for Unit (g·mol⁻¹)***	***GPC Calculated MW***	***Approximate Number of Repeating Units***
Catechol	RT Heated Layered	-$BH_2OC_6H_4O$-	127.85	2428 2550 3439	19 20 27
Phloroglucinol	RT Heated Layered	-$BH_2OC_6H_3O_2$-	142.83	1708 2633 3119	12 18 22

Table S3: Comparison of Catechol and Phloroglucinol GPC Calculated Molecular Weights and Approximate Number of Repeating Units

Thermal Analysis

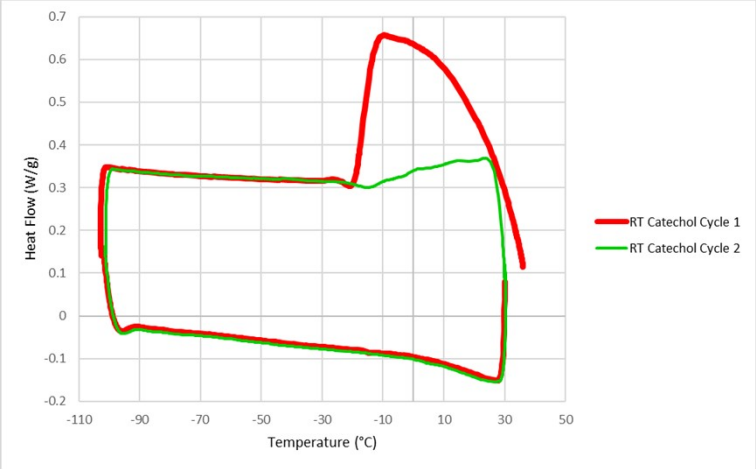

Figure S10: DSC of Room Temperature-dried Catechol Borohydride Polymer **3-O**.

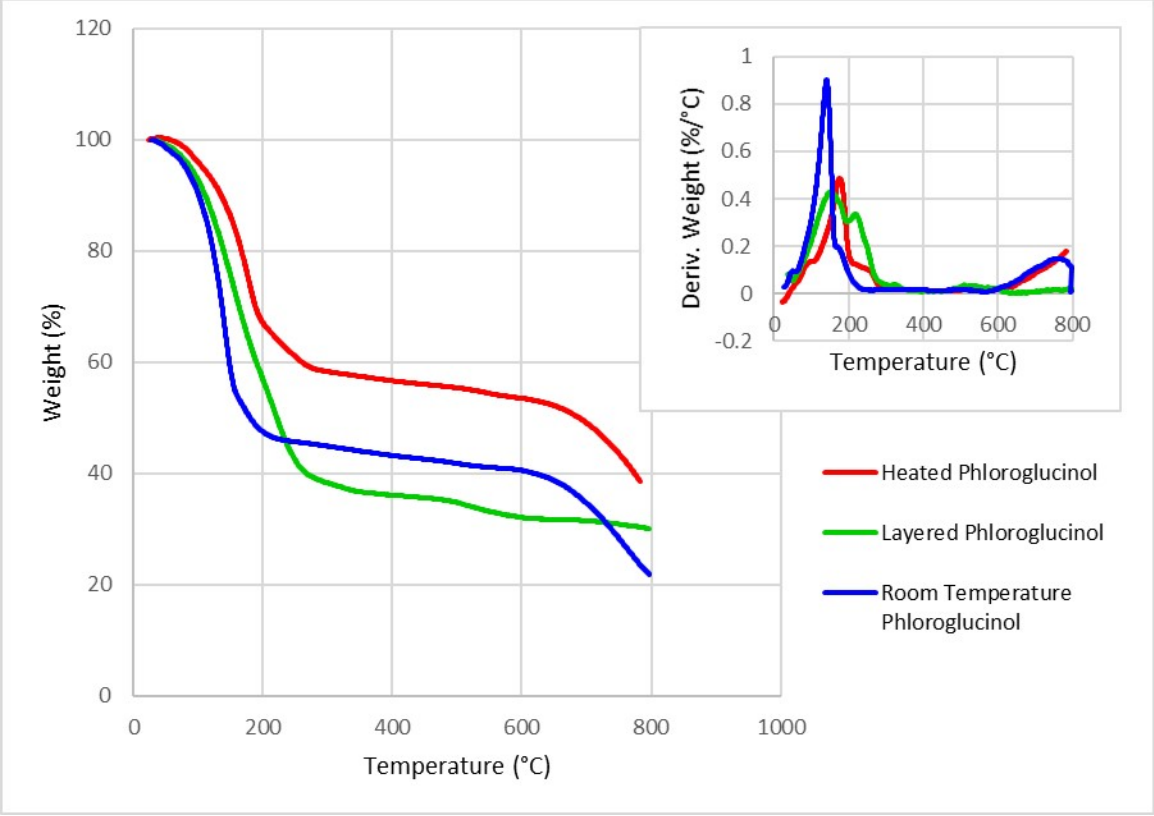

Figure S11 TGA of **3-O** from various reaction conditions, Inset: First derivative plots.

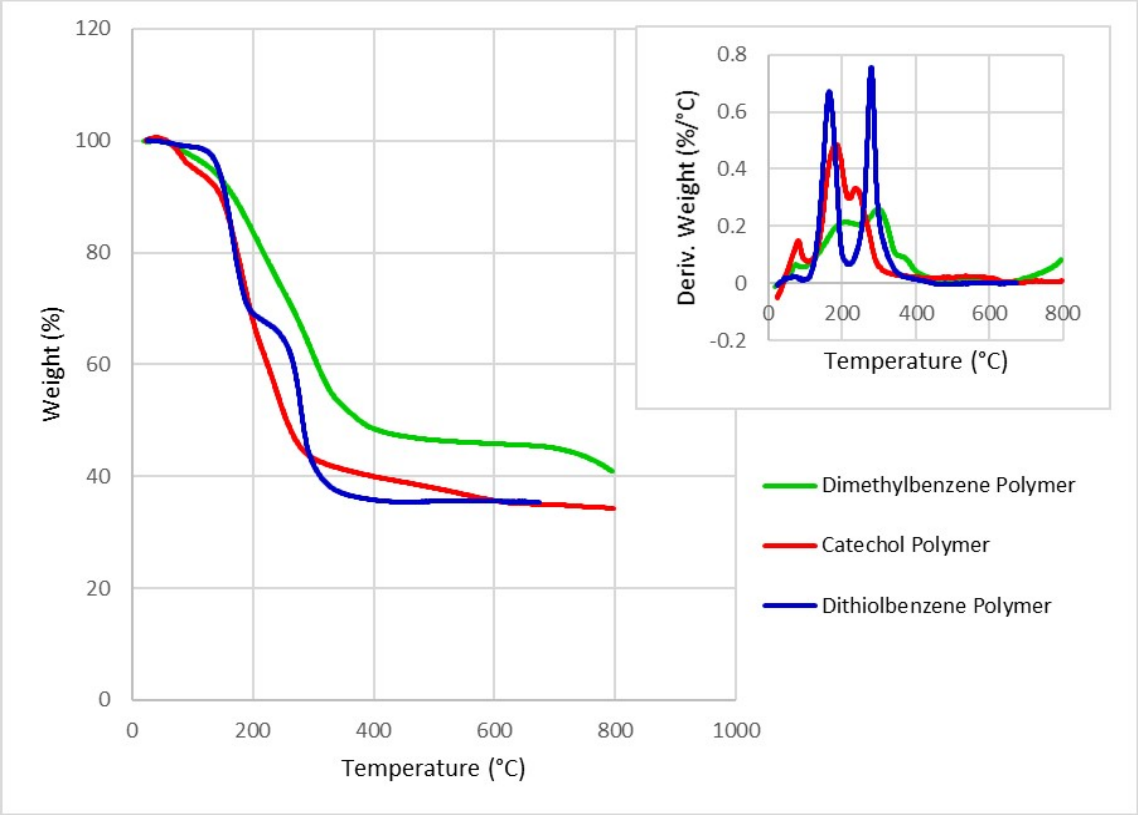

Figure S12. Comparison of TGA from **3-O**, **3-S**, and **3-CH_2** Inset: First derivative plots.

Electrochemical Impedance Spectroscopy

Polymer	***Method***	***Ionic Conductivity ($S \cdot cm^{-1}$) 60°C | 10°C (*20°C)***	***Sample Thickness (cm)***	***Activation Energy ($kJ \cdot mol^{-1}$) Cool | Heat***
3-O	Vacuum Only Heat & Vac.	3.7×10^{-7} | $1.5 \times 10^{-8*}$ 2.2×10^{-5} | 1.5×10^{-8}	0.010 0.006	110 | 120 110 | 115
4-O	Heat & Vac.	1.1×10^{-7} | $7.9 \times 10^{-10*}$	0.005	79 | 63
3-S	Heat & Vac.	1.4×10^{-4} | 5.1×10^{-8}	0.012	120 | 106
3-CH_2	Heat & Vac.	3.9×10^{-8} | 1.5×10^{-10}	0.013	88 | 95

Table S4: Polymer sample thickness and activation energies

Nyquist plots

Nyquist plots were fit to the circuit in Figure S12. The bulk ionic conductivity was calculated based on the ohmic resistance found at R_2. This value is then used in the Arrhenius plots shown in Figure 3 and 4 of the main text to extract temperature-dependent conductivity and to calculate activation energies. Representative Nyquist plots are shown with the circuit fit used; occasionally lower temperatures had to be hand extrapolated due to high levels of noise within the plots. Typically R2 was the bulk resistivity component for the polymer electrolytes tested Nyquist plots of samples at the different temperatures are also given as raw data. For samples fit or within the same general grouping are shown within the matching Appendix subsection. A description of the data is shown below the plots.

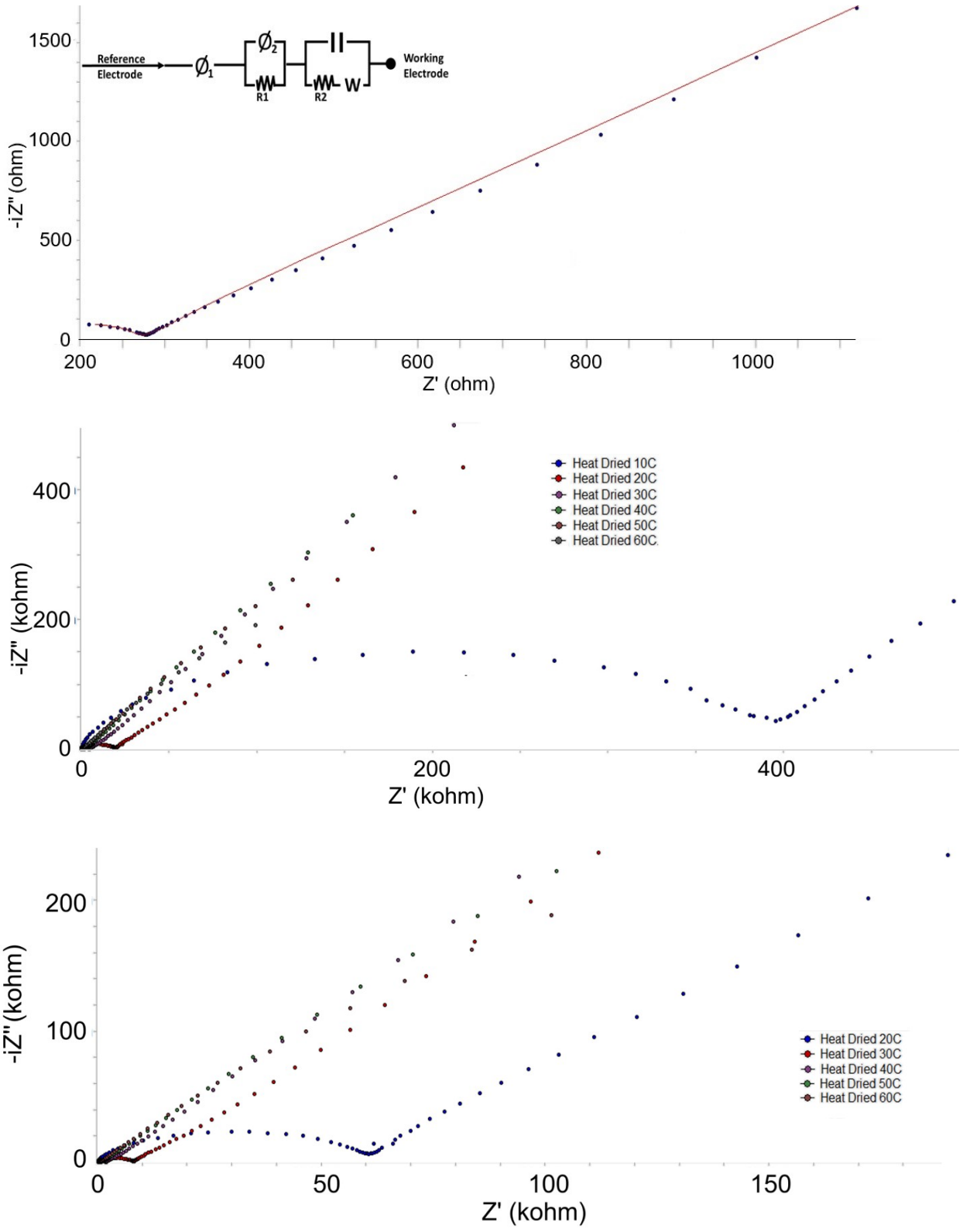

Figure S13. Heat and Vacuum Dried **3-O** Polymer at 60°C The data curves are catechol borohydride polymer heat and vacuum dried samples showing the cooling and heating cycle.

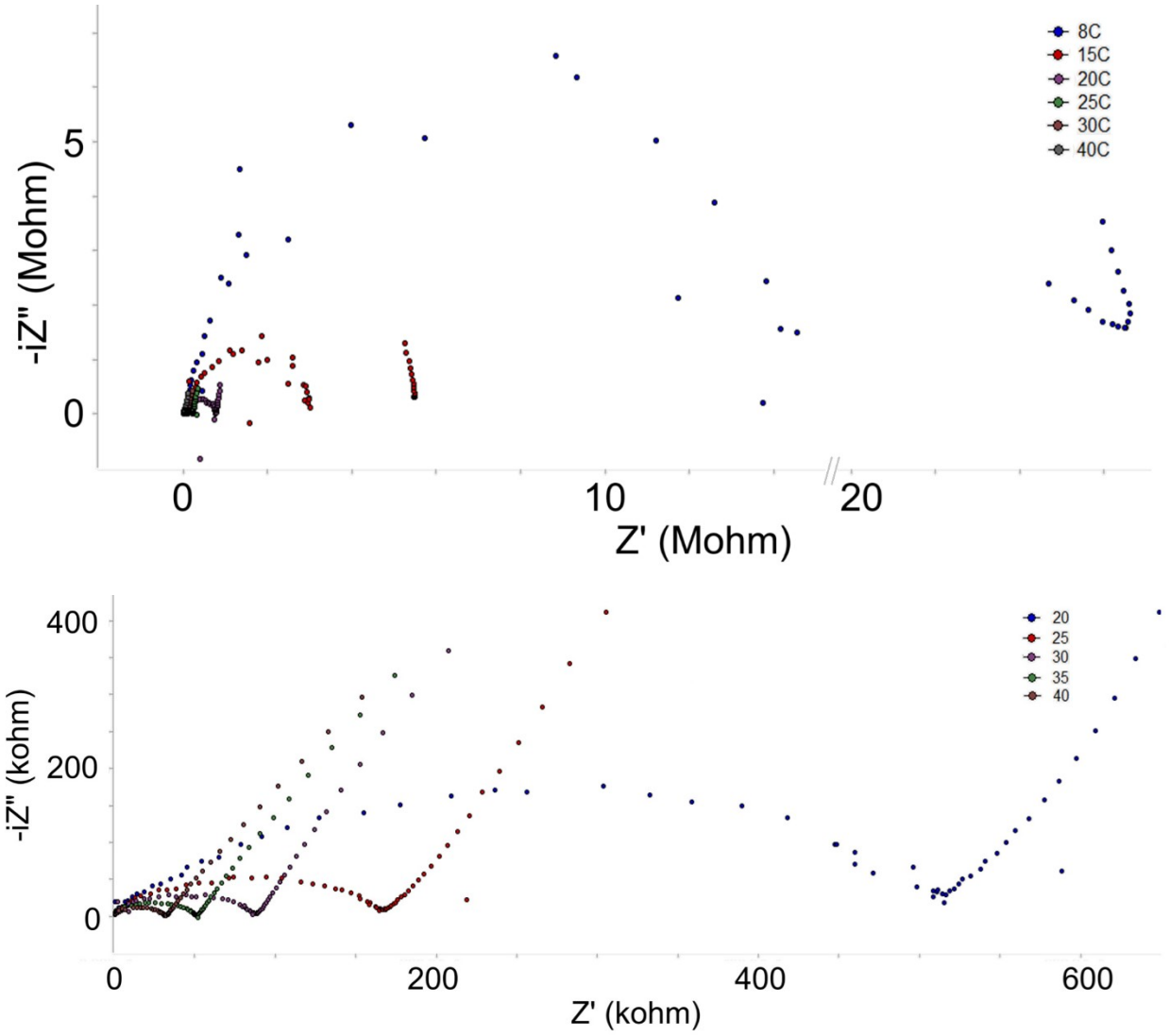

Figure S14. Nyquist plots of **3-O**. The data curves are catechol borohydride polymer vacuum dried only samples showing the cooling and heating cycles.

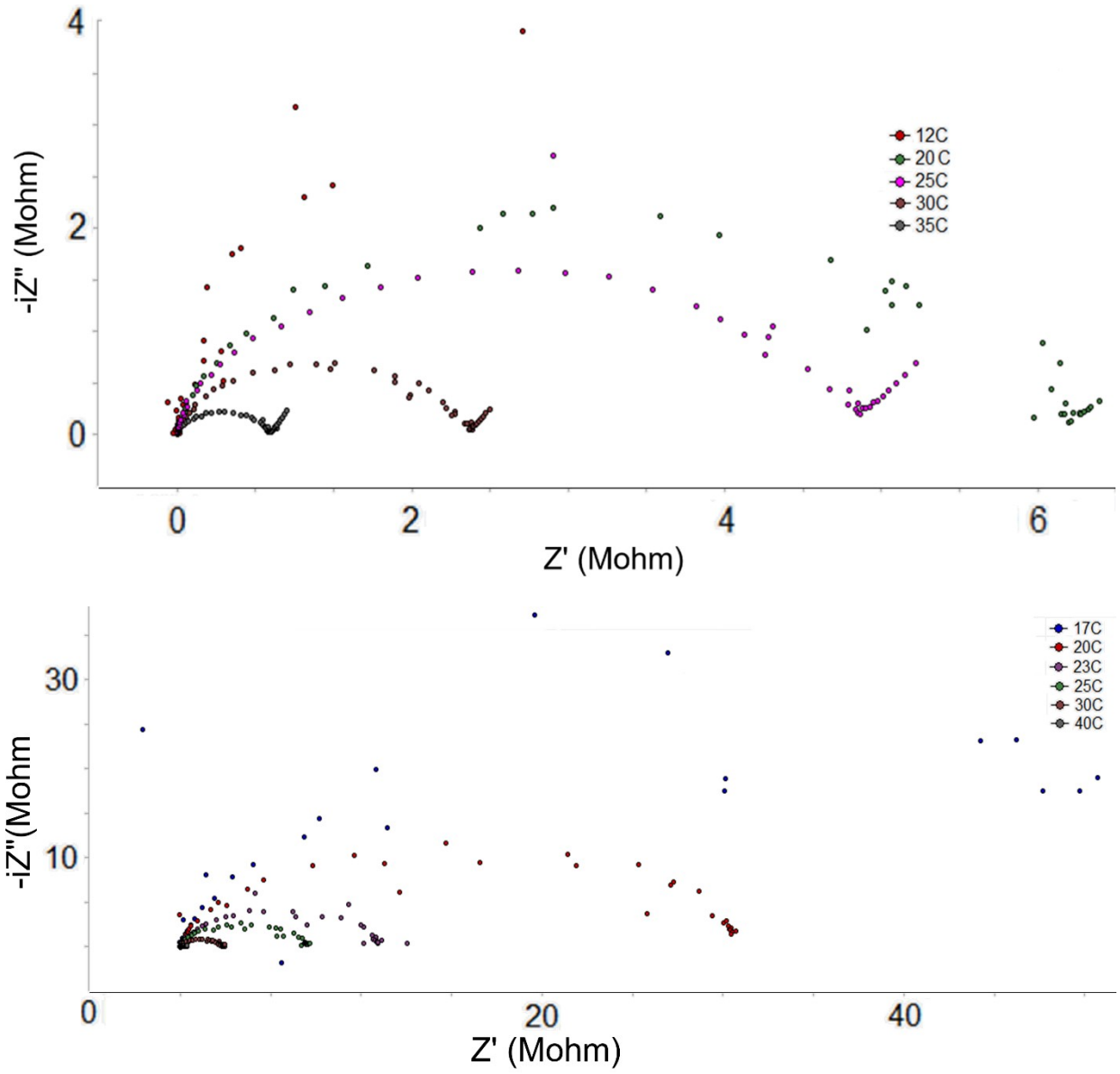

Figure S15. 3-O polymer. The data curves are catechol borohydride polymer vacuum dried only samples showing the cooling and heating cycle.

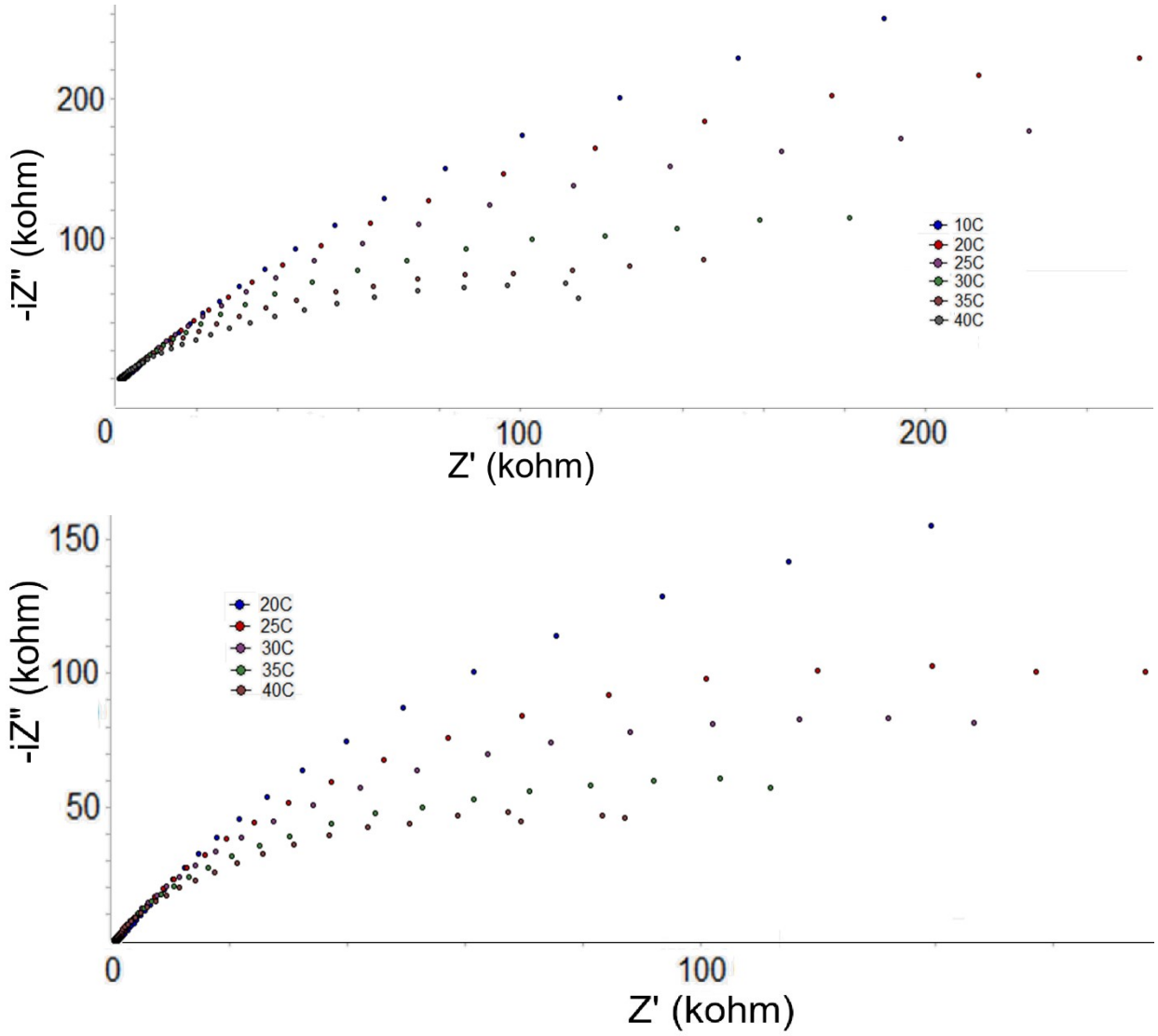

Figure S16. 3-O. The data curves are samples that were prepared by vacuum drying the catechol borohydride polymer when still suspended in solution onto a glass fiber to compare polymer EIS with an inert matrix for cooling and heating cycles.

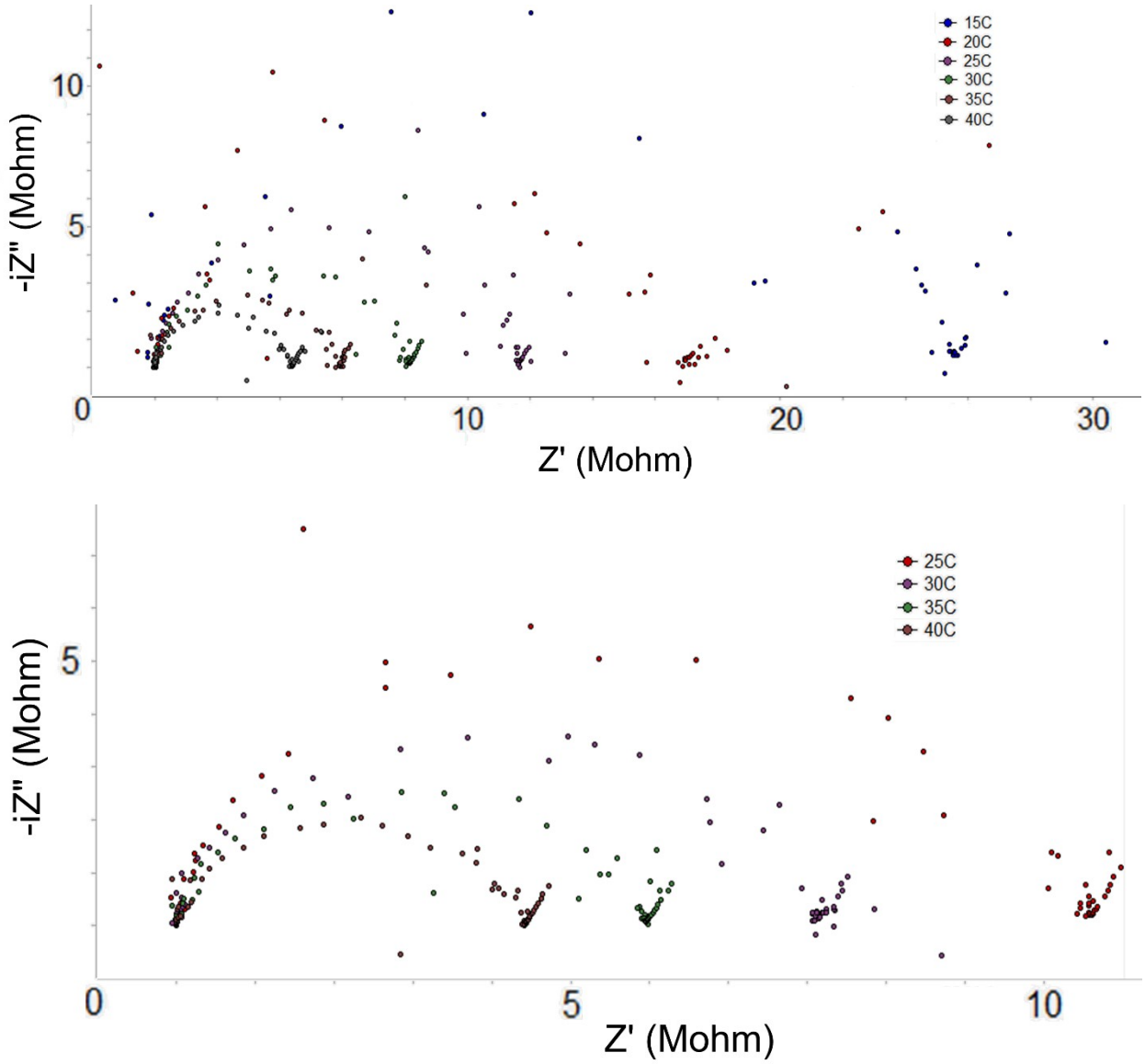

Figure S17- 3-O. The data curves are samples that were prepared by vacuum drying the catechol borohydride polymer when still suspended in solution onto a glass fiber to compare polymer EIS with an inert matrix for cooling and heating cycles.

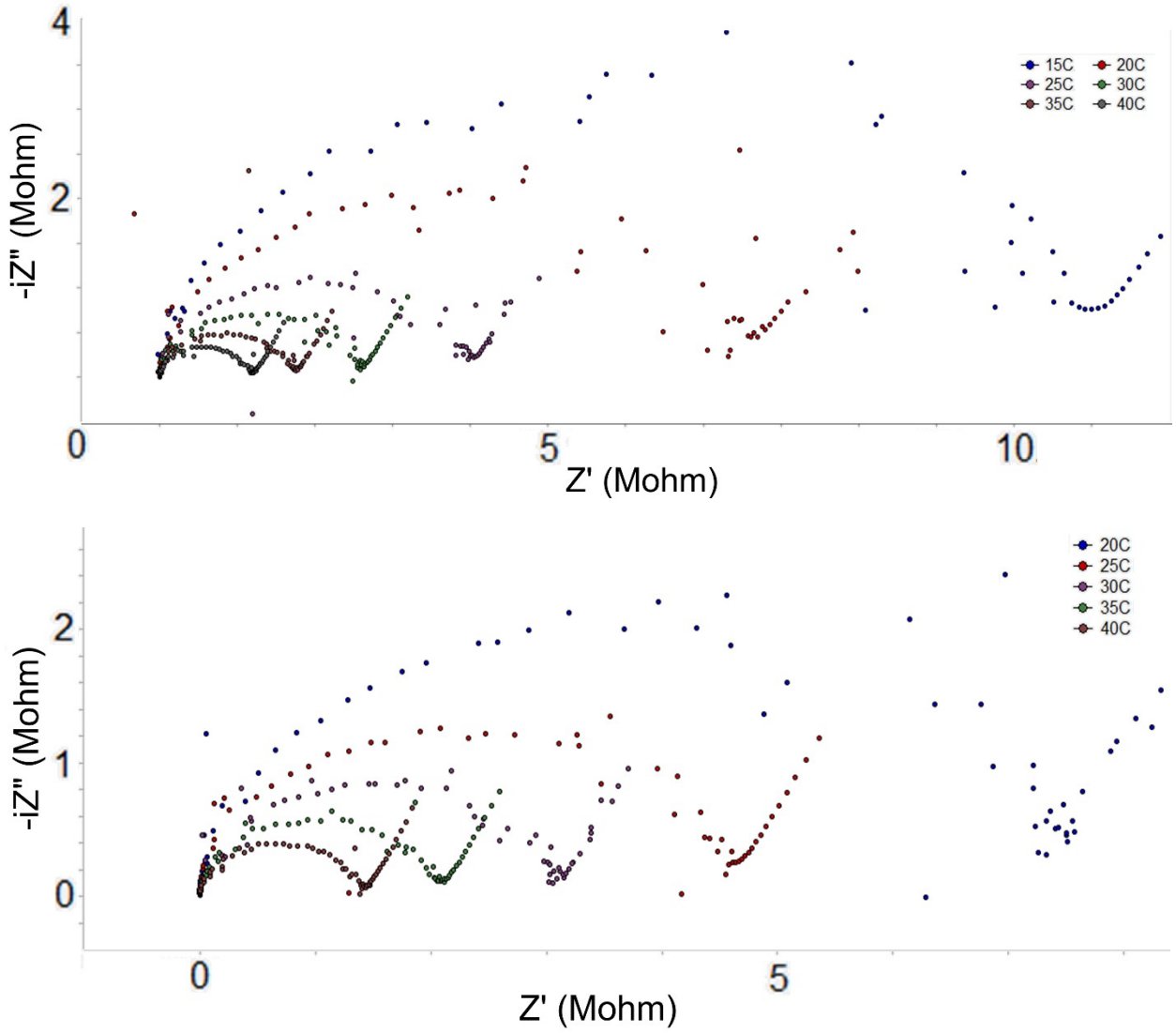

Figure S18. 3-O. The data curves are catechol borohydride polymer incorporated with lithium tetraphenylborate x 4THF and vacuum dried onto a glass fiber for cooling and heating cycles.

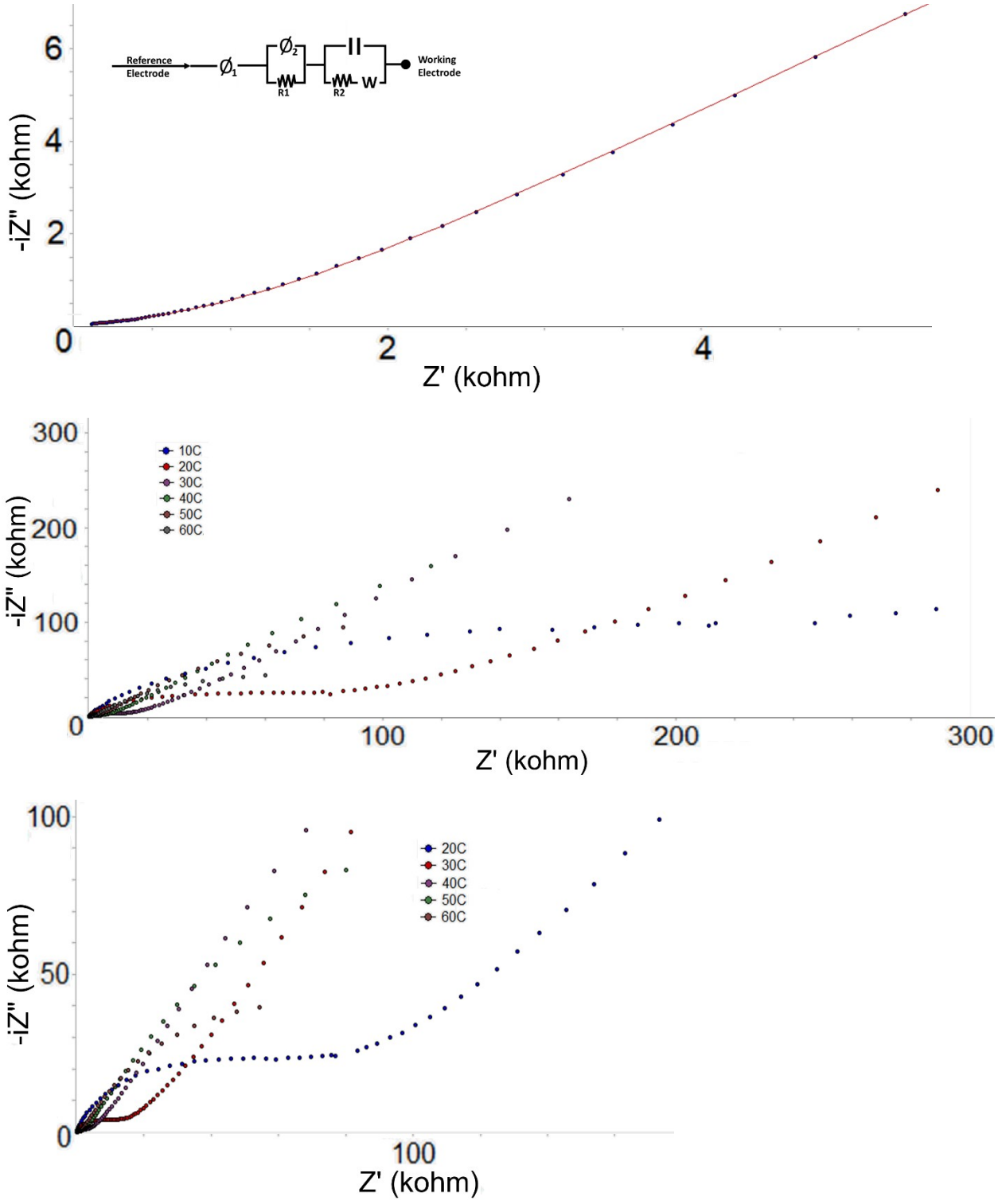

Figure S19. 3-S. The data curves are dithiobenzene borohydride polymer heat and vacuum dried sample for cooling and heating cycles.

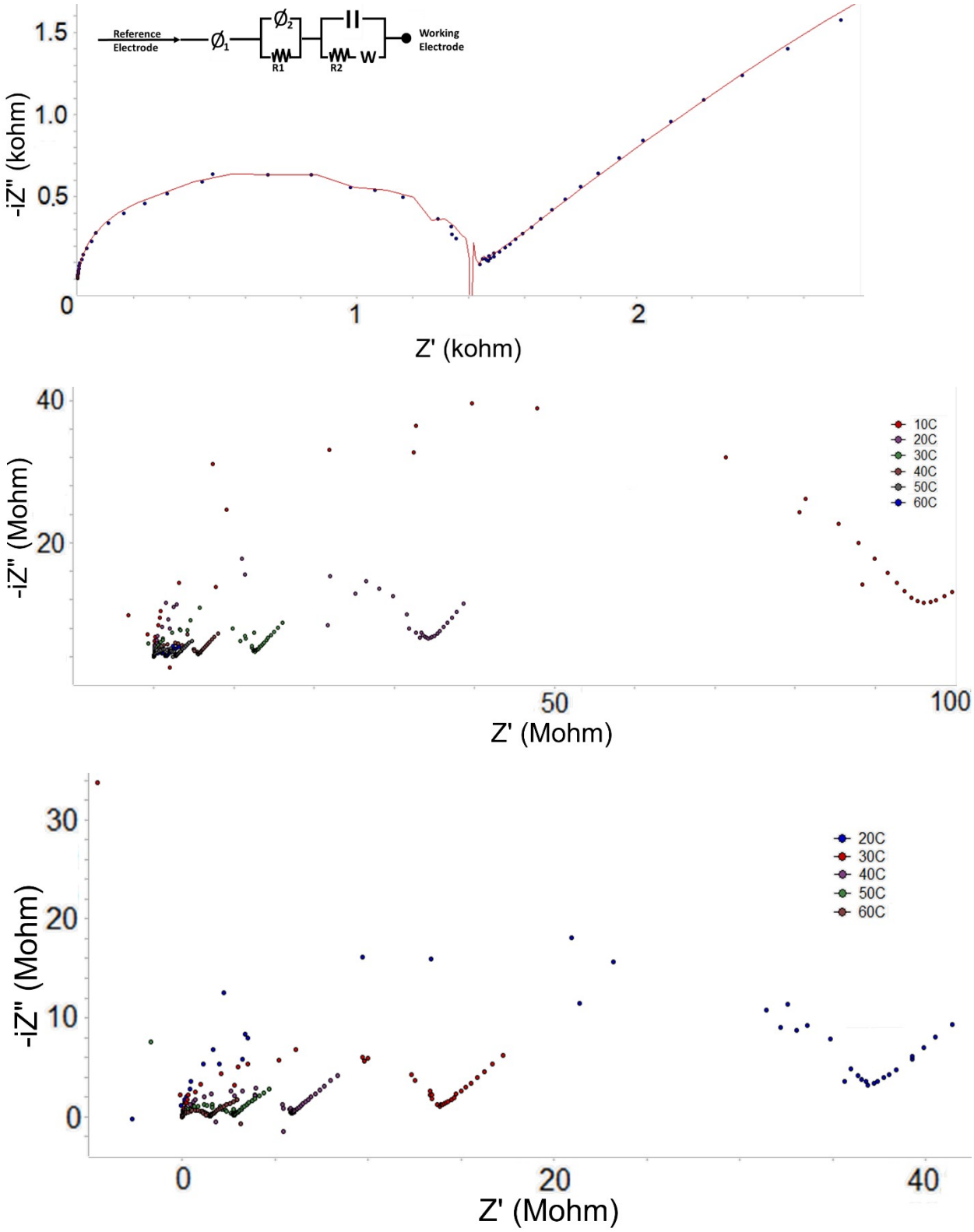

Figure S20. 3-CH_2. The data curves are dimethylbenzene borohydride polymer heat and vacuum dried sample for cooling and heating cycles.

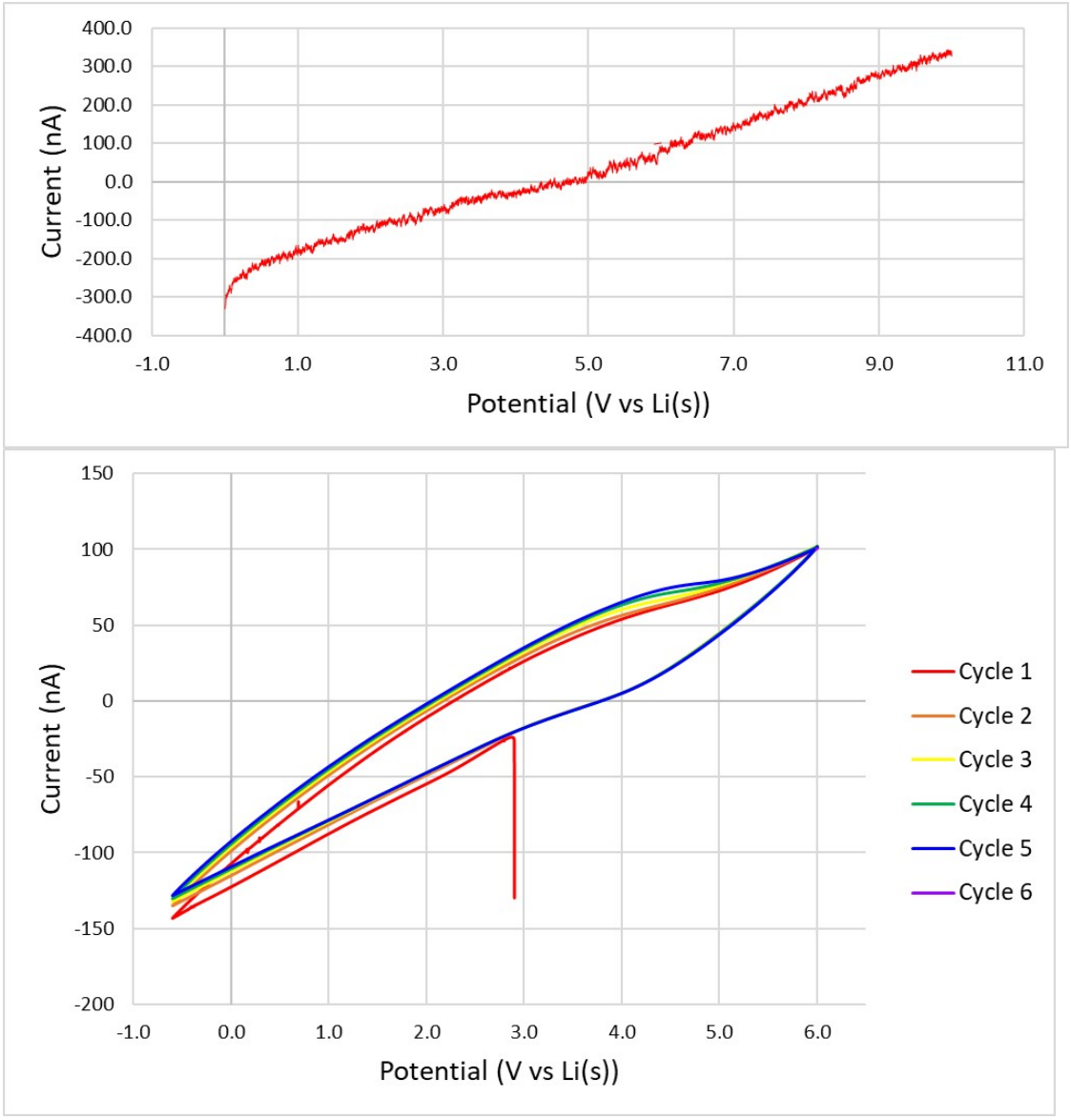

Figure S21. Volatammetry of **3-O** with Li(s) reference electrode. Top: Linear Sweep voltammetry. Bottom Cyclic Voltammetry (6 cycles). No SEI or lithium plating/stripping waves are observed, and very low current. Inactivity is attributed to decomposition of the electrolyte at Li(s).

Crystallographic Tables

$C_{58}H_{66}B_2Li_2O_6$ (**3-M**)

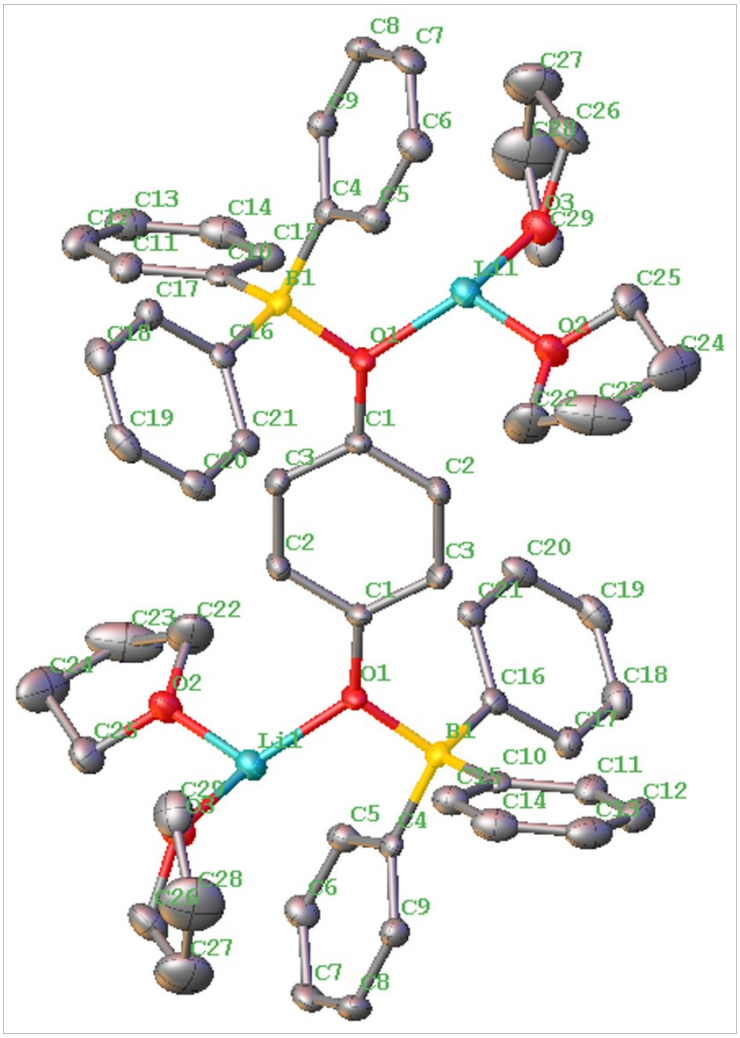

Figure S22. Thermal ellipsoid plot of 3-M with labels. Hydrogen atoms omitted for clarity.

Table S5 Crystal data and structure refinement for 3-M.

Identification code	3-M
Empirical formula	$C_{58}H_{66}B_2Li_2O_6$
Formula weight	894.60
Temperature/K	99.96
Crystal system	monoclinic
Space group	$P2_1/n$
a/Å	9.9479(4)
b/Å	10.2280(5)
c/Å	24.8303(11)
α/°	90
β/°	90.7700(10)
γ/°	90
Volume/Å^3	2526.2(2)
Z	2
ρ_{calc}g/cm^3	1.176
μ/mm^{-1}	0.073
F(000)	956.0
Crystal size/mm^3	0.188 × 0.085 × 0.065
Radiation	MoKα (λ = 0.71073)
2Θ range for data collection/°	3.28 to 53.86
Index ranges	$-12 \leq h \leq 12$, $-12 \leq k \leq 12$, $-31 \leq l \leq 31$
Reflections collected	33463
Independent reflections	4904 [R_{int} = 0.0427, R_{sigma} = 0.0411]
Data/restraints/parameters	4904/0/307
Goodness-of-fit on F^2	1.030
Final R indexes [I>=2σ (I)]	R_1 = 0.0467, wR_2 = 0.1006
Final R indexes [all data]	R_1 = 0.0821, wR_2 = 0.1162
Largest diff. peak/hole / e Å^{-3}	0.47/-0.34

Table S6 Bond Lengths for 3-M.

Atom	Atom	Length/Å	Atom	Atom	Length/Å
O1	C1	1.3724(19)	C10	C11	1.396(2)
O1	B1	1.552(2)	C10	C15	1.406(2)
O1	Li1	1.874(3)	C10	B1	1.630(3)
O2	C22	1.440(2)	C11	C12	1.392(3)
O2	C25	1.442(2)	C12	C13	1.379(3)
O2	Li1	1.900(3)	C13	C14	1.381(3)
O3	C26	1.441(2)	C14	C15	1.382(3)
O3	C29	1.434(2)	C16	C17	1.402(2)
O3	Li1	1.908(3)	C16	C21	1.400(2)
C1	C2	1.388(2)	C16	B1	1.627(3)
C1	C3[1]	1.389(2)	C17	C18	1.379(3)
C2	C3	1.387(2)	C18	C19	1.382(3)
C4	C5	1.403(2)	C19	C20	1.379(3)
C4	C9	1.395(2)	C20	C21	1.386(2)
C4	B1	1.650(2)	C22	C23	1.507(4)
C4	Li1	2.457(3)	C23	C24	1.516(4)
C5	C6	1.389(2)	C24	C25	1.496(3)
C5	Li1	2.534(3)	C26	C27	1.500(3)
C6	C7	1.379(3)	C27	C28	1.494(4)
C7	C8	1.377(3)	C28	C29	1.501(3)
C8	C9	1.397(2)	B1	Li1	2.755(3)

[1]1-X,1-Y,1-Z

Table S7 Bond Angles for 3-M.

Atom	Atom	Atom	Angle/°	Atom	Atom	Atom	Angle/°
C1	O1	B1	124.49(12)	C18	C17	C16	122.51(18)
C1	O1	Li1	128.80(13)	C17	C18	C19	120.68(18)
B1	O1	Li1	106.68(13)	C20	C19	C18	118.50(17)
C22	O2	C25	110.41(16)	C19	C20	C21	120.54(18)
C22	O2	Li1	123.09(15)	C20	C21	C16	122.43(17)
C25	O2	Li1	121.23(14)	O2	C22	C23	104.98(18)
C26	O3	Li1	123.25(14)	C22	C23	C24	103.30(18)
C29	O3	C26	106.82(15)	C25	C24	C23	101.8(2)
C29	O3	Li1	125.95(15)	O2	C25	C24	104.34(17)
O1	C1	C2	117.80(14)	O3	C26	C27	104.22(17)
O1	C1	C3[1]	124.09(15)	C28	C27	C26	105.4(2)
C2	C1	C3[1]	118.09(15)	C27	C28	C29	105.8(2)
C3	C2	C1	121.47(15)	O3	C29	C28	105.85(18)
C2	C3	C1[1]	120.43(15)	O1	B1	C4	102.60(12)
C5	C4	B1	120.29(15)	O1	B1	C10	108.85(13)
C5	C4	Li1	76.70(12)	O1	B1	C16	109.95(14)
C9	C4	C5	115.60(15)	O1	B1	Li1	40.66(9)
C9	C4	B1	124.11(15)	C4	B1	Li1	61.95(10)
C9	C4	Li1	111.82(13)	C10	B1	C4	110.97(14)
B1	C4	Li1	81.71(11)	C10	B1	Li1	121.54(13)
C4	C5	Li1	70.70(12)	C16	B1	C4	108.09(13)
C6	C5	C4	122.76(17)	C16	B1	C10	115.59(14)
C6	C5	Li1	114.72(13)	C16	B1	Li1	121.59(14)
C7	C6	C5	119.70(18)	O1	Li1	O2	116.87(16)
C8	C7	C6	119.59(17)	O1	Li1	O3	123.63(17)
C7	C8	C9	120.13(17)	O1	Li1	C4	69.00(10)
C4	C9	C8	122.20(17)	O1	Li1	C5	88.56(12)
C11	C10	C15	114.84(17)	O1	Li1	B1	32.66(7)
C11	C10	B1	125.33(16)	O2	Li1	O3	104.63(15)
C15	C10	B1	119.83(15)	O2	Li1	C4	127.63(16)
C12	C11	C10	122.72(18)	O2	Li1	C5	95.87(14)
C13	C12	C11	120.40(19)	O2	Li1	B1	130.08(15)
C12	C13	C14	118.73(19)	O3	Li1	C4	113.39(15)
C13	C14	C15	120.28(19)	O3	Li1	C5	124.46(15)
C14	C15	C10	123.04(18)	O3	Li1	B1	125.21(16)
C17	C16	B1	120.78(15)	C4	Li1	C5	32.60(7)
C21	C16	C17	115.25(16)	C4	Li1	B1	36.34(7)
C21	C16	B1	123.85(15)	C5	Li1	B1	59.97(8)

[1]1-X,1-Y,1-Z

$C_{58}H_{66}B_2Li_2O_6 \cdot 2\ C_6H_6$ (**3-M**$\cdot 2\ C_6H_6$)

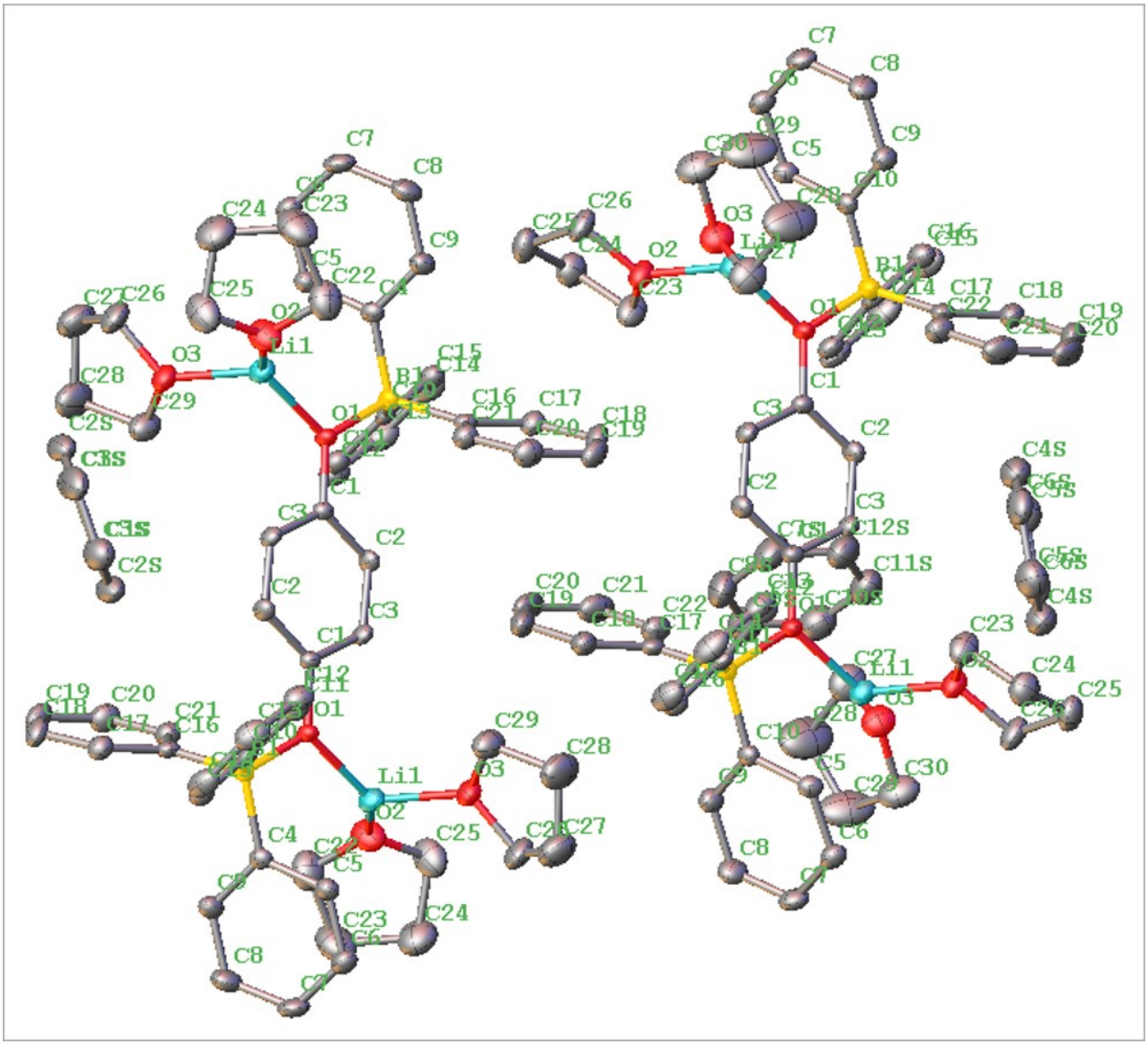

Figure S23. Thermal ellipsoid plot of 3-M$\cdot 2\ C_6H_6$ with labels. Hydrogen atoms omitted for clarity.

Table S8 Crystal data and structure refinement for 3-M·2 C_6H_6.

Identification code	3-M·2 C_6H_6.
Empirical formula	$C_{70}H_{78}B_2Li_2O_6$
Formula weight	1050.82
Temperature/K	100.03
Crystal system	triclinic
Space group	P-1
a/Å	11.2628(17)
b/Å	13.699(2)
c/Å	20.426(3)
α/°	98.899(4)
β/°	104.077(4)
γ/°	92.733(4)
Volume/Å^3	3008.1(8)
Z	2
ρ_{calc}g/cm^3	1.160
μ/mm^{-1}	0.071
F(000)	1124.0
Crystal size/mm^3	0.28 × 0.12 × 0.085
Radiation	MoKα (λ = 0.71073)
2Θ range for data collection/°	2.086 to 50.122
Index ranges	$-13 \le h \le 13$, $-16 \le k \le 16$, $-24 \le l \le 24$
Reflections collected	77261
Independent reflections	10495 [R_{int} = 0.0511, R_{sigma} = 0.0323]
Data/restraints/parameters	10495/0/721
Goodness-of-fit on F^2	1.017
Final R indexes [I>=2σ (I)]	R_1 = 0.0484, wR_2 = 0.1188
Final R indexes [all data]	R_1 = 0.0709, wR_2 = 0.1327
Largest diff. peak/hole / e Å^{-3}	0.67/-0.33

Table S9 Bond Lengths for 3-M·2 C_6H_6.

Atom	Atom	Length/Å	Atom	Atom	Length/Å
O1_1	C1_1	1.374(2)	O3_2	C30_2	1.433(3)
O1_1	B1_1	1.548(2)	O3_2	Li1_2	1.903(3)
O1_1	Li1_1	1.873(3)	C1_2	C2_2	1.391(2)
O2_1	C22_1	1.442(3)	C1_2	C3_2[2]	1.390(2)
O2_1	C25_1	1.425(3)	C1S_2	C2S_2	1.380(3)
O2_1	Li1_1	1.906(3)	C1S_2	C3S_2[3]	1.381(3)
O3_1	C26_1	1.439(2)	C2_2	C3_2	1.387(2)
O3_1	C29_1	1.444(2)	C2S_2	C3S_2	1.375(4)
O3_1	Li1_1	1.914(3)	C4S_2	C5S_2	1.379(4)
C1_1	C2_1	1.391(2)	C4S_2	C6S_2[4]	1.375(4)
C1_1	C3_1	1.389(2)	C5_2	C6_2	1.388(2)
C2_1	C3_1[1]	1.385(2)	C5_2	C10_2	1.409(2)
C4_1	C5_1	1.409(2)	C5_2	Li1_2	2.480(4)
C4_1	C9_1	1.400(2)	C5S_2	C6S_2	1.372(4)
C4_1	B1_1	1.646(2)	C6_2	C7_2	1.384(3)
C4_1	Li1_1	2.633(4)	C7_2	C8_2	1.381(3)
C5_1	C6_1	1.388(2)	C7S_2	C8S_2	1.376(4)
C5_1	Li1_1	2.476(4)	C7S_2	C12S_2	1.373(4)
C6_1	C7_1	1.383(3)	C8_2	C9_2	1.388(3)
C7_1	C8_1	1.385(3)	C8S_2	C9S_2	1.379(4)
C8_1	C9_1	1.390(3)	C9_2	C10_2	1.400(2)
C10_1	C11_1	1.399(3)	C9S_2	C10S_2	1.371(4)
C10_1	C15_1	1.400(2)	C10_2	B1_2	1.647(3)
C10_1	B1_1	1.631(3)	C10_2	Li1_2	2.556(4)
C11_1	C12_1	1.386(3)	C10S_2	C11S_2	1.376(4)
C12_1	C13_1	1.378(3)	C11_2	C12_2	1.399(3)
C13_1	C14_1	1.381(3)	C11_2	C16_2	1.402(3)
C14_1	C15_1	1.388(3)	C11_2	B1_2	1.630(3)
C16_1	C17_1	1.395(3)	C11S_2	C12S_2	1.376(4)
C16_1	C21_1	1.403(3)	C12_2	C13_2	1.392(3)
C16_1	B1_1	1.635(3)	C13_2	C14_2	1.380(3)
C17_1	C18_1	1.394(3)	C14_2	C15_2	1.379(3)
C18_1	C19_1	1.379(3)	C15_2	C16_2	1.389(3)
C19_1	C20_1	1.381(3)	C17_2	C18_2	1.395(3)
C20_1	C21_1	1.385(3)	C17_2	C22_2	1.403(3)
C22_1	C23_1	1.508(3)	C17_2	B1_2	1.633(3)
C23_1	C24_1	1.513(4)	C18_2	C19_2	1.397(3)
C24_1	C25_1	1.505(3)	C19_2	C20_2	1.375(4)
C26_1	C27_1	1.505(3)	C20_2	C21_2	1.378(4)

Table S9 Bond Lengths for 3-M·2 C_6H_6.

Atom	Atom	Length/Å	Atom	Atom	Length/Å
C27_1	C28_1	1.480(3)	C21_2	C22_2	1.384(3)
C28_1	C29_1	1.500(3)	C23_2	C24_2	1.517(3)
O1_2	C1_2	1.370(2)	C24_2	C25_2	1.511(3)
O1_2	B1_2	1.547(2)	C25_2	C26_2	1.513(3)
O1_2	Li1_2	1.876(3)	C27_2	C28_2	1.474(4)
O2_2	C23_2	1.447(2)	C28_2	C29_2	1.522(4)
O2_2	C26_2	1.441(2)	C29_2	C30_2	1.506(4)
O2_2	Li1_2	1.897(3)	B1_2	Li1_2	2.819(4)
O3_2	C27_2	1.443(3)			

[1]-X,1-Y,1-Z; [2]1-X,1-Y,2-Z; [3]-1-X,1-Y,1-Z; [4]2-X,1-Y,2-Z

Table S10 Bond Angles for 3-M·2 C_6H_6.

Atom	Atom	Atom	Angle/°	Atom	Atom	Atom	Angle/°
C1_1	O1_1	B1_1	123.78(13)	C3_2[2]	C1_2	C2_2	118.19(16)
C1_1	O1_1	Li1_1	123.26(14)	C2S_2	C1S_2	C3S_2[3]	120.1(2)
B1_1	O1_1	Li1_1	111.97(14)	C3_2	C2_2	C1_2	120.58(16)
C22_1	O2_1	Li1_1	126.44(16)	C3S_2	C2S_2	C1S_2	120.1(2)
C25_1	O2_1	C22_1	104.53(16)	C2_2	C3_2	C1_2[2]	121.22(16)
C25_1	O2_1	Li1_1	125.19(17)	C2S_2	C3S_2	C1S_2[3]	119.8(2)
C26_1	O3_1	C29_1	108.85(15)	C6S_2[4]	C4S_2	C5S_2	120.1(2)
C26_1	O3_1	Li1_1	123.07(15)	C6_2	C5_2	C10_2	122.68(17)
C29_1	O3_1	Li1_1	121.63(14)	C6_2	C5_2	Li1_2	113.91(14)
O1_1	C1_1	C2_1	123.84(15)	C10_2	C5_2	Li1_2	76.72(12)
O1_1	C1_1	C3_1	118.02(14)	C6S_2	C5S_2	C4S_2	120.4(3)
C3_1	C1_1	C2_1	118.13(15)	C7_2	C6_2	C5_2	119.90(17)
C3_1[1]	C2_1	C1_1	120.47(16)	C5S_2	C6S_2	C4S_2[4]	119.6(2)
C2_1[1]	C3_1	C1_1	121.40(15)	C8_2	C7_2	C6_2	119.09(17)
C5_1	C4_1	B1_1	120.82(15)	C12S_2	C7S_2	C8S_2	119.8(3)
C5_1	C4_1	Li1_1	67.94(12)	C7_2	C8_2	C9_2	120.62(18)
C9_1	C4_1	C5_1	115.45(16)	C7S_2	C8S_2	C9S_2	120.5(2)
C9_1	C4_1	B1_1	123.70(16)	C8_2	C9_2	C10_2	122.23(18)
C9_1	C4_1	Li1_1	125.27(14)	C10S_2	C9S_2	C8S_2	119.8(3)
B1_1	C4_1	Li1_1	79.59(11)	C5_2	C10_2	B1_2	120.15(15)
C4_1	C5_1	Li1_1	80.23(12)	C5_2	C10_2	Li1_2	70.83(12)
C6_1	C5_1	C4_1	122.80(17)	C9_2	C10_2	C5_2	115.42(16)
C6_1	C5_1	Li1_1	117.95(14)	C9_2	C10_2	B1_2	124.42(16)
C7_1	C6_1	C5_1	119.70(18)	C9_2	C10_2	Li1_2	117.13(14)
C6_1	C7_1	C8_1	119.40(17)	B1_2	C10_2	Li1_2	81.14(12)
C7_1	C8_1	C9_1	120.26(18)	C9S_2	C10S_2	C11S_2	119.6(3)
C8_1	C9_1	C4_1	122.33(18)	C12_2	C11_2	C16_2	115.45(17)
C11_1	C10_1	C15_1	115.14(16)	C12_2	C11_2	B1_2	124.11(16)
C11_1	C10_1	B1_1	124.19(16)	C16_2	C11_2	B1_2	120.42(16)
C15_1	C10_1	B1_1	120.59(16)	C12S_2	C11S_2	C10S_2	120.7(2)
C12_1	C11_1	C10_1	122.74(18)	C13_2	C12_2	C11_2	122.53(19)
C13_1	C12_1	C11_1	120.55(19)	C7S_2	C12S_2	C11S_2	119.7(3)
C12_1	C13_1	C14_1	118.41(18)	C14_2	C13_2	C12_2	120.1(2)
C13_1	C14_1	C15_1	120.71(18)	C15_2	C14_2	C13_2	119.23(19)
C14_1	C15_1	C10_1	122.42(18)	C14_2	C15_2	C16_2	120.2(2)
C17_1	C16_1	C21_1	115.63(17)	C15_2	C16_2	C11_2	122.48(19)
C17_1	C16_1	B1_1	124.67(16)	C18_2	C17_2	C22_2	115.24(18)
C21_1	C16_1	B1_1	119.60(16)	C18_2	C17_2	B1_2	124.83(18)
C18_1	C17_1	C16_1	122.29(18)	C22_2	C17_2	B1_2	119.93(17)
C19_1	C18_1	C17_1	120.39(18)	C17_2	C18_2	C19_2	122.1(2)

Table S10 Bond Angles for 3-M·2 C_6H_6.

Atom	Atom	Atom	Angle/°	Atom	Atom	Atom	Angle/°
C18_1	C19_1	C20_1	118.82(18)	C20_2	C19_2	C18_2	120.7(2)
C19_1	C20_1	C21_1	120.44(19)	C19_2	C20_2	C21_2	118.9(2)
C20_1	C21_1	C16_1	122.42(18)	C20_2	C21_2	C22_2	120.1(2)
O2_1	C22_1	C23_1	105.32(19)	C21_2	C22_2	C17_2	123.0(2)
C22_1	C23_1	C24_1	105.02(19)	O2_2	C23_2	C24_2	105.45(16)
C25_1	C24_1	C23_1	103.2(2)	C25_2	C24_2	C23_2	101.81(17)
O2_1	C25_1	C24_1	103.85(18)	C24_2	C25_2	C26_2	102.30(17)
O3_1	C26_1	C27_1	105.60(18)	O2_2	C26_2	C25_2	105.31(16)
C28_1	C27_1	C26_1	102.5(2)	O3_2	C27_2	C28_2	104.8(2)
C27_1	C28_1	C29_1	103.5(2)	C27_2	C28_2	C29_2	104.3(2)
O3_1	C29_1	C28_1	105.83(17)	C30_2	C29_2	C28_2	105.2(2)
O1_1	B1_1	C4_1	103.37(13)	O3_2	C30_2	C29_2	105.8(2)
O1_1	B1_1	C10_1	110.40(14)	O1_2	B1_2	C10_2	102.07(13)
O1_1	B1_1	C16_1	108.89(14)	O1_2	B1_2	C11_2	110.53(15)
C10_1	B1_1	C4_1	107.87(14)	O1_2	B1_2	C17_2	109.46(14)
C10_1	B1_1	C16_1	115.62(14)	O1_2	B1_2	Li1_2	38.57(9)
C16_1	B1_1	C4_1	109.98(14)	C10_2	B1_2	Li1_2	63.60(11)
O1_1	Li1_1	O2_1	127.01(18)	C11_2	B1_2	C10_2	108.53(14)
O1_1	Li1_1	O3_1	113.87(16)	C11_2	B1_2	C17_2	114.24(15)
O1_1	Li1_1	C4_1	65.07(10)	C11_2	B1_2	Li1_2	119.10(13)
O1_1	Li1_1	C5_1	86.83(13)	C17_2	B1_2	C10_2	111.33(15)
O2_1	Li1_1	O3_1	111.43(16)	C17_2	B1_2	Li1_2	124.90(14)
O2_1	Li1_1	C4_1	106.84(14)	O1_2	Li1_2	O2_2	114.73(16)
O2_1	Li1_1	C5_1	113.27(15)	O1_2	Li1_2	O3_2	126.94(18)
O3_1	Li1_1	C4_1	126.39(16)	O1_2	Li1_2	C5_2	88.05(13)
O3_1	Li1_1	C5_1	97.24(14)	O1_2	Li1_2	C10_2	66.15(11)
C5_1	Li1_1	C4_1	31.83(7)	O1_2	Li1_2	B1_2	30.94(7)
C1_2	O1_2	B1_2	124.47(13)	O2_2	Li1_2	O3_2	108.22(16)
C1_2	O1_2	Li1_2	124.36(14)	O2_2	Li1_2	C5_2	97.79(14)
B1_2	O1_2	Li1_2	110.49(14)	O2_2	Li1_2	C10_2	127.92(16)
C23_2	O2_2	Li1_2	122.77(14)	O2_2	Li1_2	B1_2	126.16(15)
C26_2	O2_2	C23_2	109.56(14)	O3_2	Li1_2	C5_2	115.82(15)
C26_2	O2_2	Li1_2	123.75(15)	O3_2	Li1_2	C10_2	109.07(15)
C27_2	O3_2	Li1_2	122.65(16)	O3_2	Li1_2	B1_2	125.59(15)
C30_2	O3_2	C27_2	106.52(16)	C5_2	Li1_2	C10_2	32.45(7)
C30_2	O3_2	Li1_2	127.70(16)	C5_2	Li1_2	B1_2	59.63(9)
O1_2	C1_2	C2_2	123.95(15)	C10_2	Li1_2	B1_2	35.26(7)
O1_2	C1_2	C3_2[2]	117.86(15)				

[1]-X,1-Y,1-Z; [2]1-X,1-Y,2-Z; [3]-1-X,1-Y,1-Z; [4]2-X,1-Y,2-Z